SIMULATION STUDY OF AREAL SWEEP EFFICIENCY VERSUS A FUNCTION OF MOBILITY RATIO AND ASPECT RATIO FOR STAGGERED LINE-DRIVE WATERFLOOD PATTERN

A Thesis

by

RUSLAN GULIYEV

Submitted to the Office of Graduate Studies of
Texas A&M University
in partial fulfillment of the requirements for the degree of

MASTER OF SCIENCE

August 2008

Major Subject: Petroleum Engineering

SIMULATION STUDY OF AREAL SWEEP EFFICIENCY VERSUS A FUNCTION OF MOBILITY RATIO AND ASPECT RATIO FOR STAGGERED LINE-DRIVE WATERFLOOD PATTERN

A Thesis

by

RUSLAN GULIYEV

Submitted to the Office of Graduate Studies of
Texas A&M University
in partial fulfillment of the requirements for the degree of

MASTER OF SCIENCE

Approved by:

Chair of Committee,	Daulat D. Mamora
Committee Members,	Jerome J. Schubert
	Luc T. Ikelle
Head of Department,	Stephen A. Holditch

August 2008

Major Subject: Petroleum Engineering

ABSTRACT

Simulation Study of Areal Sweep Efficiency Versus a Function
of Mobility Ratio and Aspect Ratio for Staggered
Line-drive Waterflood Pattern. (August 2008)
Ruslan Guliyev, B.S., Azerbaijan State Oil Academy
Chair of Advisory Committee: Dr. Daulat D. Mamora

Pattern geometry plays a major role in determining oil recovery during waterflooding and enhanced oil recovery operations. Although simulation is an important tool for design and evaluation, the first step often involves rough calculations based upon areal sweep efficiencies of displacements in homogeneous, two-dimensional, scaled, physical models. These results are available as a function of the displacement pattern and the mobility ratio **M**.

In this research I studied the effect of mobility ratios on five-spot and staggered waterflood patterns behavior for areal (2D) displacement in a reservoir that is homogeneous and isotropic containing no initial gas saturation. Simulation was performed using Eclipse 100 simulator.

Simulation results are presented as graphs of areal sweep efficiency at breakthrough versus Craig mobility ratio for various staggered line drive aspect ratios.

The main results of the study are presented in the form of a graph of areal sweep efficiency at breakthrough as a function of staggered line drive aspect ratio. This should enable engineers to utilize the results in a convenient manner.

ACKNOWLEDGEMENTS

I wish to express my sincere gratitude and appreciation to Dr. Daulat D. Mamora, chair of my advisory committee, for his patience and continued support throughout my research. I would also like to thank Dr. Jerome Schubert, member of my advisory committee, for his encouragement to my research, his motivation and his “always-good mood”. I also acknowledge Dr. Luc Ikelle, member of my advisory committee, for his participation and guidance during my investigation. Finally, I want to express my gratitude and appreciation to all my colleagues in Texas A&M University: Samir Husseynzade, Faig Hasanov, and Mazen Barnawi.

TABLE OF CONTENTS

CHAPTER Page

LIST OF FIGURES

FIGURE Page

FIGURE Page

CHAPTER I
INTRODUCTION

1.1 Well patterns and mobility ratio

There are several basic well patterns that are commonly used waterfloods, as listed below (Fig. 1.1). Each pattern results in unique waterflood performance: Four Spot; Five Spot; Seven Spot; Nine Spot; Direct Line Drive; Staggered Line Drive.

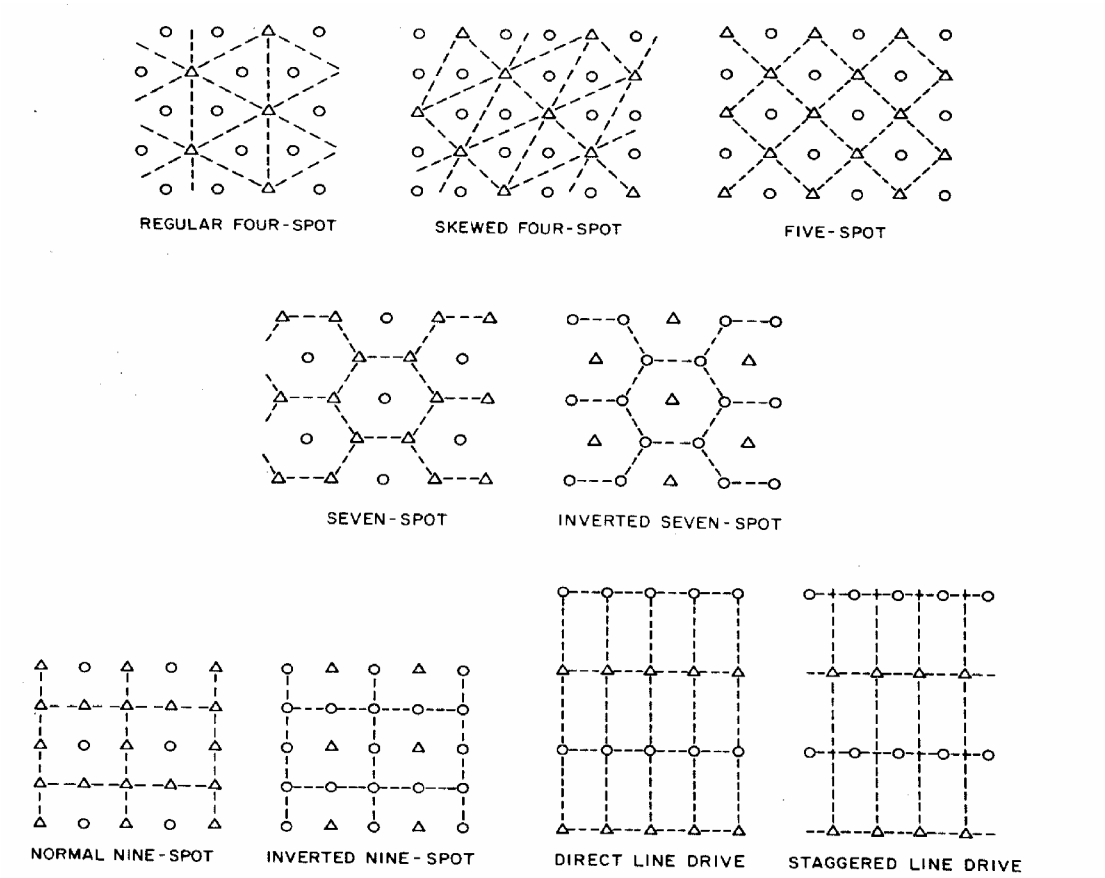

Figure 1.1 Illustration of waterflood patterns (Craig, F.F. Jr. 1971)

This thesis follows the style of *SPE Journal.*

In a waterflood, water is injected in a well or pattern of wells to displace oil towards a producer. When the leading edge of the waterflood front reaches the producer breakthrough occurs (the first appearance of water in the produced fluids). After breakthrough, both oil and water are produced and the watercut increases progressively.

The main objective of enhanced oil recovery (EOR) is to economically increase displacement and areal sweep efficiency. A key factor is the mobility ratio - ***M***.

The mobility ratio is simply the ratio of the mobility of the displacing phase to that of the displaced or resident phase.

$$\boldsymbol{M}_{ep} = \frac{k_{rwe}}{\mu_w}\frac{\mu_o}{k_{roe}} \qquad \ldots\ldots\ldots\ldots\ldots\ldots\ldots\ldots (1.1)$$

Where $\boldsymbol{M_{ep}}$ is end point mobility ratio; k_{rwe} and k_{roe} are end point relative permeability for water and oil respectively; μ_o and μ_w are water and oil insitu viscosities. Mobility ratio is a function of viscosity and relative permeability, which in turn depends on saturation. A variation of mobility ratio is Craig's mobility ratio - $\boldsymbol{M}_{\mathbf{c}}$, defined as:

$$\boldsymbol{M_c} = \frac{k_{rw}(\overline{S_w})}{\mu_w}\frac{\mu_o}{k_{ro}} \qquad \ldots\ldots\ldots\ldots\ldots\ldots\ldots\ldots (1.2)$$

Where $k_{rw}(\overline{\mathrm{S_w}})$ is the water relative permeability at the average saturation behind the flood front.

1.2 Areal sweep efficiency

For piston-like displacement, the areal sweep efficiency is:

$$E_A = A_S / A_T \qquad \ldots\ldots\ldots\ldots\ldots\ldots\ldots\ldots (1.3)$$

Where A_S is the swept area and A_T is the total area. Before and at breakthrough, the amount of displacing fluid injected is equal to the displaced fluid produced, disregarding compressibility. Assuming piston-like displacement, injected volume is related to area swept.

$$Wi = A_S h\phi(1 - S_{wc} - S_{or}) \quad \ldots\ldots\ldots\ldots\ldots\ldots\ldots \quad (1.4)$$

Where W_i is the volume of displacing fluid injected, h is the thickness of the formation, and ϕ is porosity. Hence,

$$E_A = A_S / A_T = Wi / (A_T h\phi(1 - S_{wc} - S_{or})) \quad \ldots\ldots\ldots\ldots \quad (1.5)$$

After breakthrough,

$$E_A = (W_i - W_P) / (A_T h\phi(1 - S_{wc} - S_{or})) \quad \ldots\ldots\ldots\ldots \quad (1.6)$$

Where W_P is volume of displacing fluid produced.

1.3 Displacement in a five-spot pattern

Analysis of a five-spot pattern in a reservoir can be simplified by examining the behavior of a single five-spot pattern. A regular five-spot pattern consists of a production well surrounded by four injection wells. It is assumed that the injection rates are equal to the production rates. Thus flow is symmetric around each injection well with 0.25 of the injection rate from each well confined to the pattern (Fig. 1.2).

Further simplifications are possible. A line drawn from injection well to production well subdivides a quadrant into two symmetrical parts. Thus displacement performance of one-eighth of a five-spot pattern is used to estimate the behavior of the full pattern. In simulation, use of one-eight model will result in significant saving in CPU time.

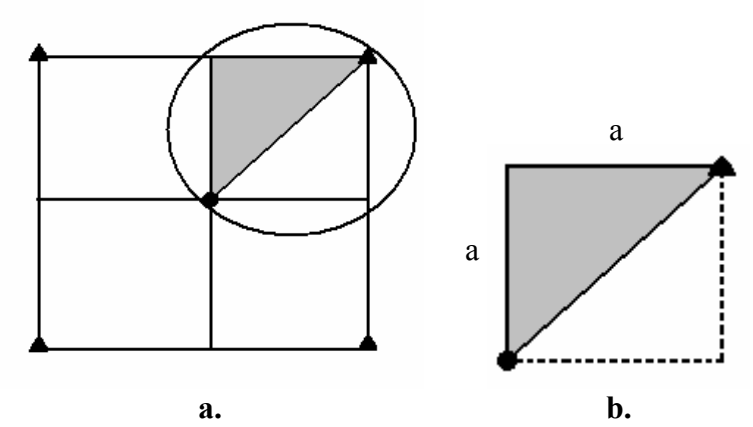

Figure 1.2 Single five-spot pattern (a), one-eight of a five-spot pattern (shaded) (b)

Areal sweep efficiency and oil recovery efficiency at breakthrough are readily determined from the correlations that have been developed from experiments with scaled laboratory models.

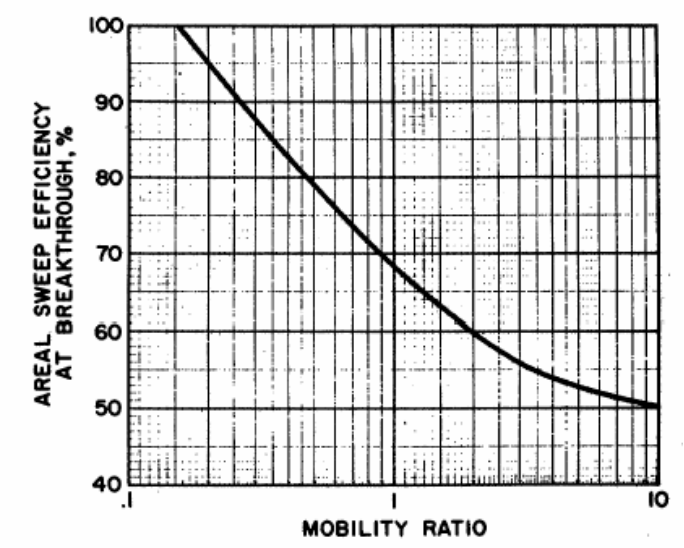

Figure 1.3 Correlation of areal sweep efficiency as a function of Craig water oil mobility ratio for five-spot patterns (Forrest F. Craig. Jr. 1971)

A convenient way of estimating E_{Abt} is to use the expression for the correlation graphed in Fig. 1.3, which is as follows.

$$E_{Abt} = 0.54602036 + \frac{0.03170817}{M_c} + \frac{0.30222997}{e^{M_c}} - 0.00509693 M_c \ldots \quad (1.7)$$

1.4 Displacement in a staggered pattern

Similar mapping can be seen in a staggered line drive pattern. As well as five-spot pattern it has an injection well surrounded by four production wells but the distance between them is not equally distributed (see Fig. 1.4 a.). Simplified pattern becomes one-eight of staggered line drive pattern presented in Fig. 1.4 b. Consequently, models of displacement performances in staggered pattern refer to an ideal five-spot pattern where aspect ratio d/a exists.

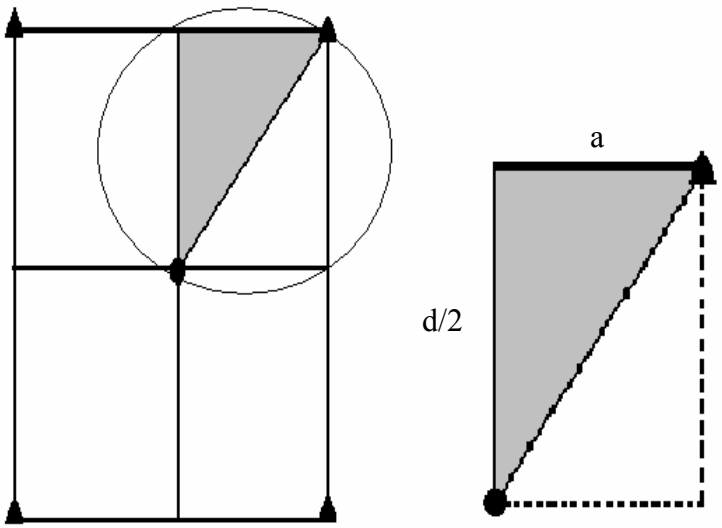

Figure 1.4 Single staggered line-drive pattern (a), and simplified one-eighth of a staggered line-drive pattern (shaded) (b)

CHAPTER II
LITERATURE REVIEW

Not many studies were directed to develop relations between areal sweep efficiency and reservoir or fluid characterization parameters especially for different staggered pattern distribution. Most notable works on staggered line drive are described below.

2.1 Pitts, Gerald N., Crawford, Paul B. 1971, Simulating large flow networks in underground media

This study describes the possible effect of heterogeneous media on the areal sweep efficiencies for different pattern distributions. The direct streamline method was applied to three well known reservoir patterns: five-spot, direct-line drive (square) and staggered line drive patterns. Each pattern was simulated with three different permeability ranges. The ranges were (a) 100 to 50 md, (b) 100 to 1.0 md and (c) 100 to 0. 1 md. These distributions were used along with a random process to distribute the permeabilities throughout a 20 x 20 matrix yielding a 400 block system.

It was found that areal sweeps for very heterogeneous five-spot patterns were reduced to nearly 25 percent or about one-third of the sweep expected in homogeneous media.

The heterogeneous staggered line drive pattern gave surprisingly low areal sweeps, the average areal sweep for the (100 to 50) md range was 76 percent, 65 percent for the (100 to 1.0) md range, and 26 percent sweep for the (100 to 0.1) md range. The two smaller permeability ranges resulted in a larger areal sweep for the staggered line-drive than the five-spot or direct-line drive patterns. However, for the wide permeability range of (100 to 0. 1), about the same areal sweep was obtained for the staggered-line drive and the five-spot patterns, but both gave smaller sweeps than the direct-line drive square pattern.

2.2 Brigham, William E., Kovscek, Anthony R., Wang, Yuandong 1998, A study of the effect of mobility ratios on pattern displacement behavior and streamline to infer permeability fields permeability media

In this particular research it was found that for unit mobility ratio, unfavorable mobility ratios and some favorable mobility ratios ($M > 0.3$) in a staggered line-drive pattern has higher areal sweep efficiency than a five-spot pattern. However, for very favorable mobility ratios ($M < 0.3$), a five-spot pattern has better sweep efficiency than a common staggered-line-drive. The reason for this behavior was the change of streamline and pressure distributions with mobility ratios. For very favorable mobility ratios, the displacing front is near an isobar and intersects the pattern boundary at 90 degrees. That causes the fronts at times near breakthrough to become radial around the producer for a five-spot pattern. This displacing front shape is due to the symmetry of the five-spot pattern. Also, noticed more numerical dispersion in results for unfavorable mobility ratio cases ($M > 1$).

For a staggered line drive, the displacing front is also perpendicular to the border of the pattern. However, because the pattern is not symmetric, sweepout at breakthrough is not complete. So theoretically it seems that only in the limit of very large d/a will the areal sweep efficiency approach 1.

CHAPTER III
RESEARCH OBJECTIVES

The main objective of this research is to determine the areal sweep efficiency versus mobility ratio distribution for different aspect ratios by simulating simplified (one-eight) staggered line drive patterns using Schlumberger Eclipse 100 commercial simulator. The results obtained should be useful for estimating areal sweep efficiency at breakthrough when one is designing a staggered line-drive waterflood. To determine the affect of grid number on simulation results all simulation runs will be performed for three cases where grid distributions are 20x10x1, 40x20x1 and 60x30x1 where areas for all cases are equal.

CHAPTER IV
SIMULATION AND CALCULATIONS

To simulate the displacement for the five-spot and staggered line-drive patterns we will use Eclipse 100 with a two-dimensional grid distribution.

4.1 Conditions and limitations

The main features of the simulation model and runs are as follows:

1. Two dimensional where area equal 40 acres and thickness is 20 feet.
2. Incompressible displacement.
3. Homogeneous permeability field, *i.e., k* is constant and equal 30%.
4. No gas presents initially, *Sgi*=0.
5. Constant injection and production rates, $Q_i=Q_p$.
6. Relative permeability curves described with Corey-type equations.
7. Oil to water viscosity ratio μ_o/μ_w (where μ_w =1cp) is reciprocal of oil viscosity that will have values: 0.2; 0.5; 1; 2; 3; 5 and 10 cp.
8. $1/8^{th}$ of the basic unit described by a triangular Cartesian grid block.
9. Three cases were studied: 20x10x1, 40x20x1 and 60x30x1.

4.2 Gridding

In this research I built five staggered grid patterns for each grid distribution where aspect ratio (d/a) will change linearly: 0.75; 1; 1.25; 1.5 and 1.75.

Fig. 4.1, **Fig. 4.2** and **Fig. 4.3** illustrate waterflood performance in simplified five-spot patterns for different grid distribution: 20x10x1, 40x20x1 and 60x30x1 respectively.

Fig. 4.4 through **Fig. 4.8** represent staggered patterns performance at breakthrough for finest grid distribution (60x30x1), where aspect ratio is changing from 0.75 to 1.75.

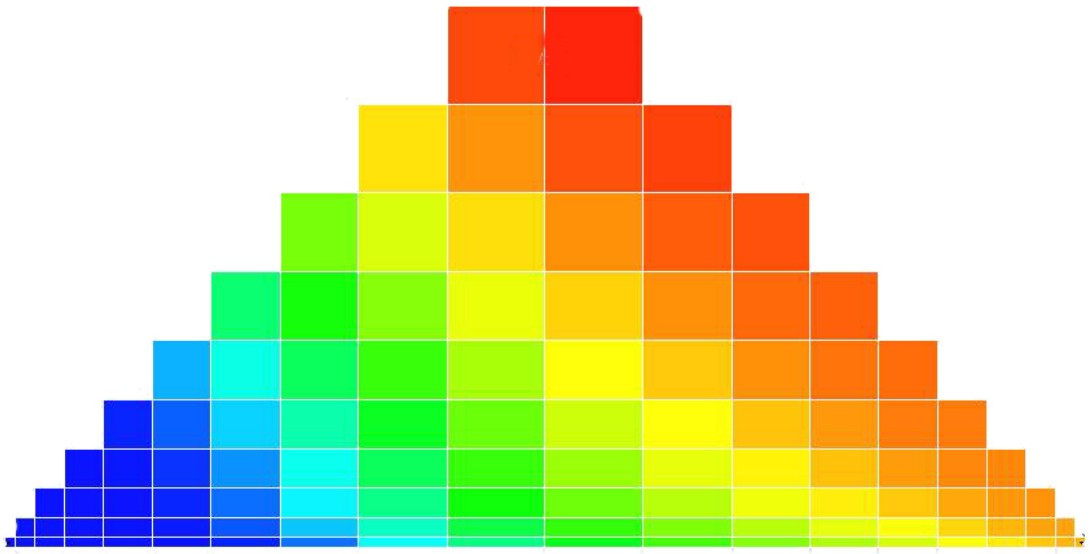

Figure 4.1 Flood performance in one-eight of five-spot pattern with 20x10x1 model

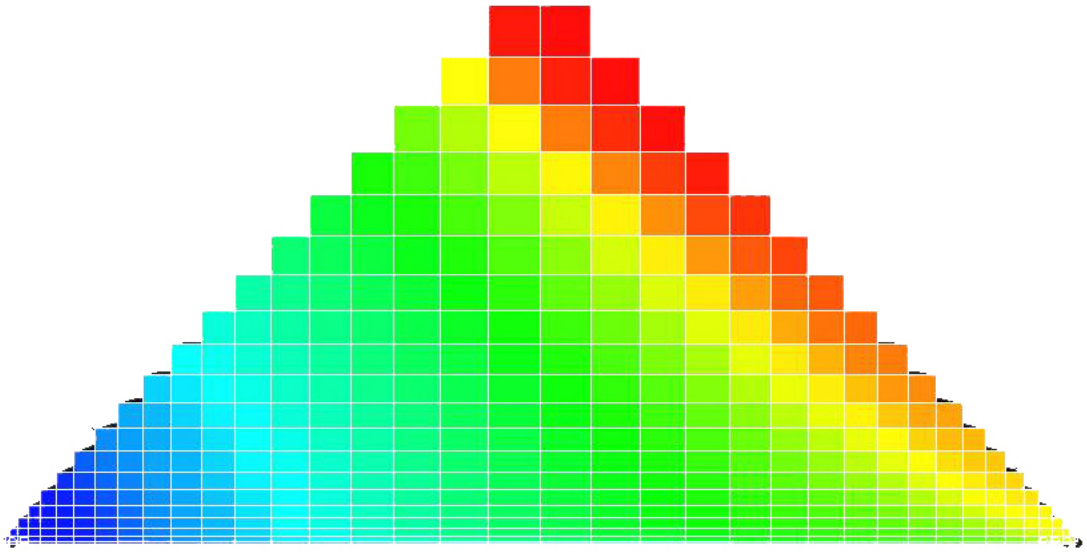

Figure 4.2 Flood performance in one-eight of five-spot pattern with 40x20x1 model

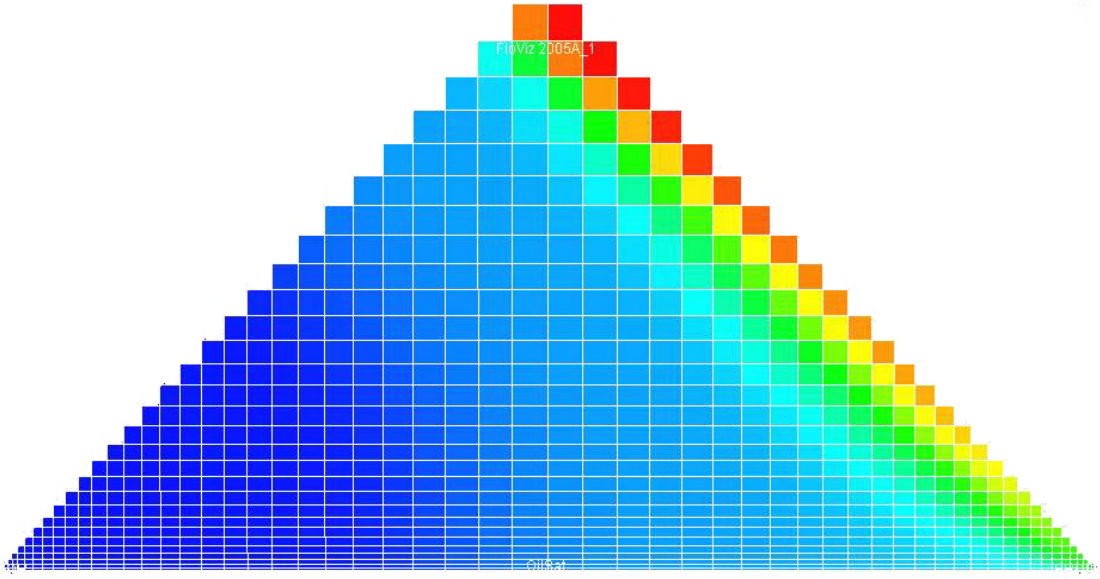

Figure 4.3 Flood performance in one-eight of five-spot pattern with 60x30x1 model

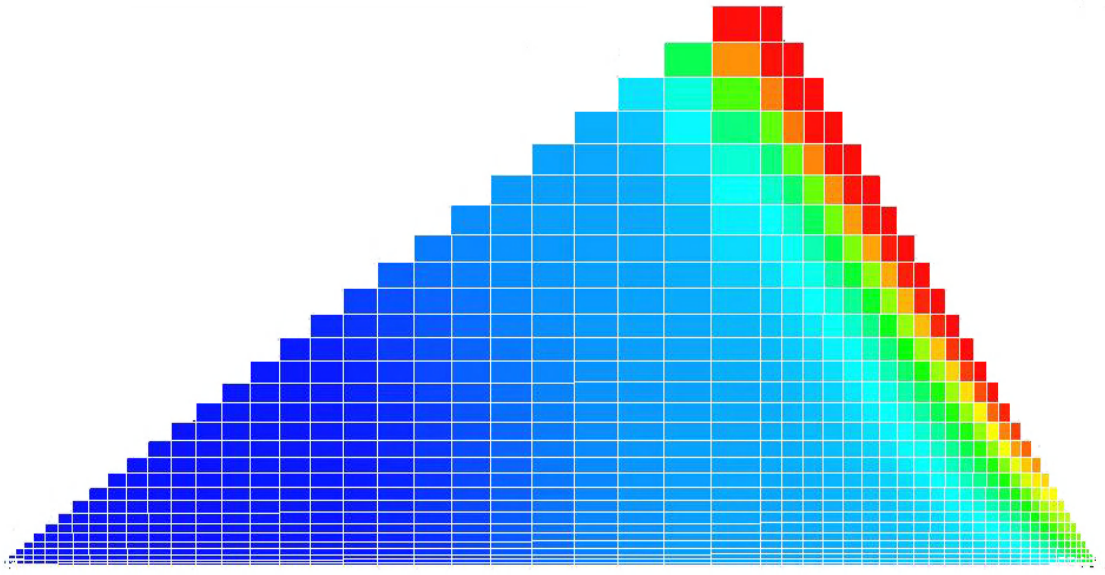

Figure 4.4 Flood performance in one-eight of staggered line-drive pattern with 60x30x1model, d/a=0.75

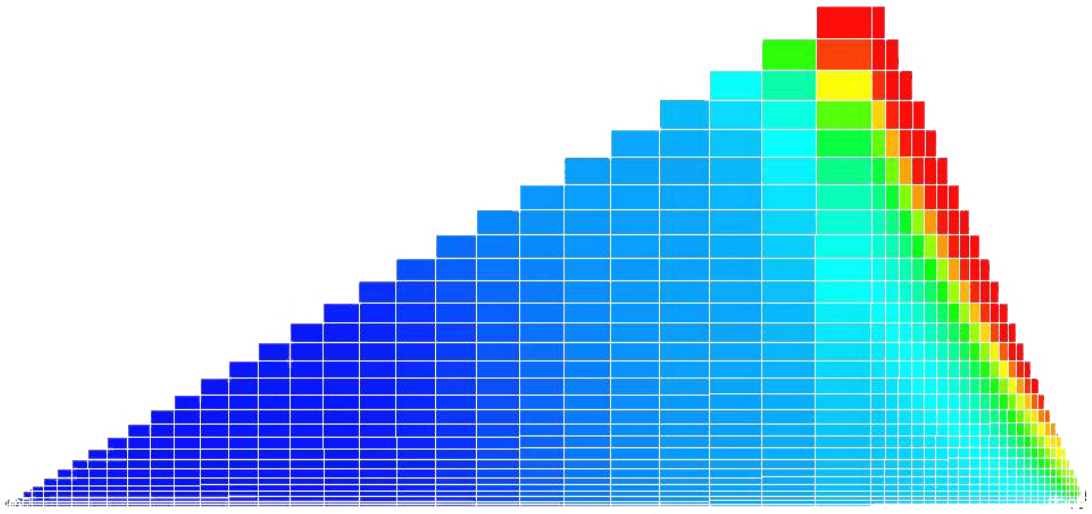

Figure 4.5 Flood performance in one-eight of staggered line-drive pattern with 60x30x1 model, d/a=1

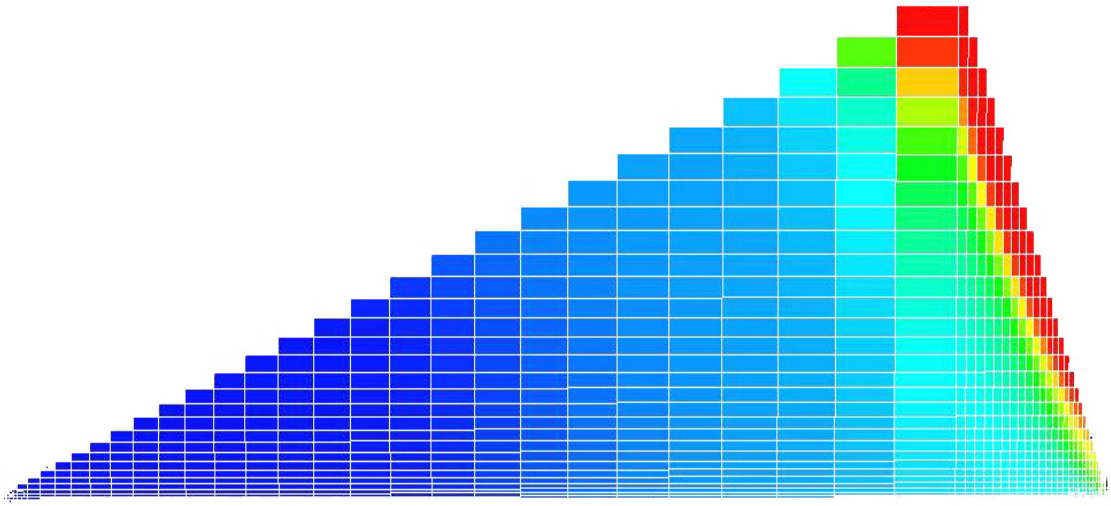

Figure 4.6 Flood performance in one-eight of staggered line-drive pattern with 60x30x1 model, d/a=1.25

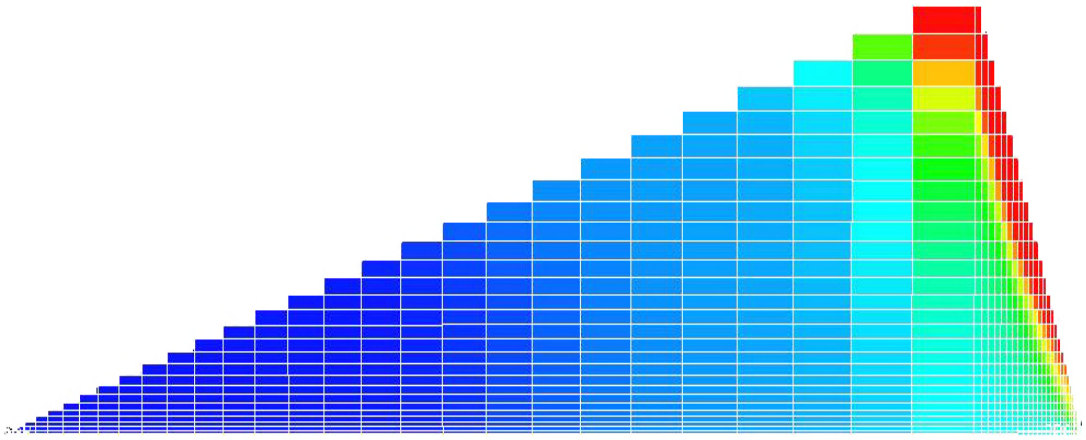

Figure 4.7 Flood performance in one-eight of staggered line-drive pattern with 60x30x1 model, d/a=1.5

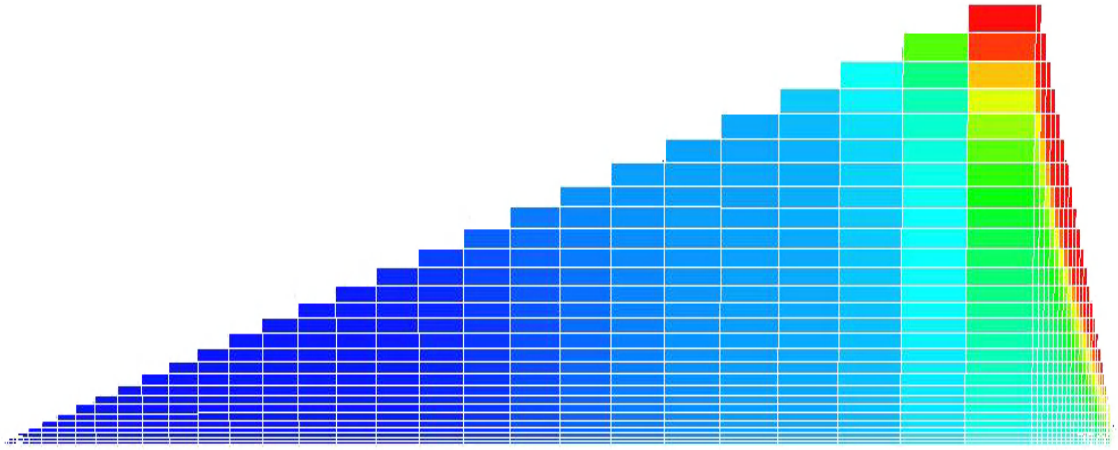

Figure 4.8 Flood performance in one-eight of staggered line-drive pattern with 60x30x1 model, d/a=1.75

4.3 Methodology

4.3.1 Oil-water relative permeability calculation

For relative permeability calculation Corey-type relative permeability curves for oil and water have been used.

For oil, $k_{ro} = (1-S_{wD})^{n_o}$,……..……..(4.1)

and for water $k_{rw} = S_{wD}^{n_w}$,……..(4.2)

where: $S_{wD} = \dfrac{(S_w - S_{wc})}{(1 - S_{wc} - S_{or})}$,……..……...…….(4.3)

In my study the following parameters were used:

$S_{wc} = 0.22$; $S_{or} = 0.20$

$n_o = 2$; $n_w = 1.8$

Using Corey equation the following relative permeability curves shown on **Fig. 4.9** were obtained.

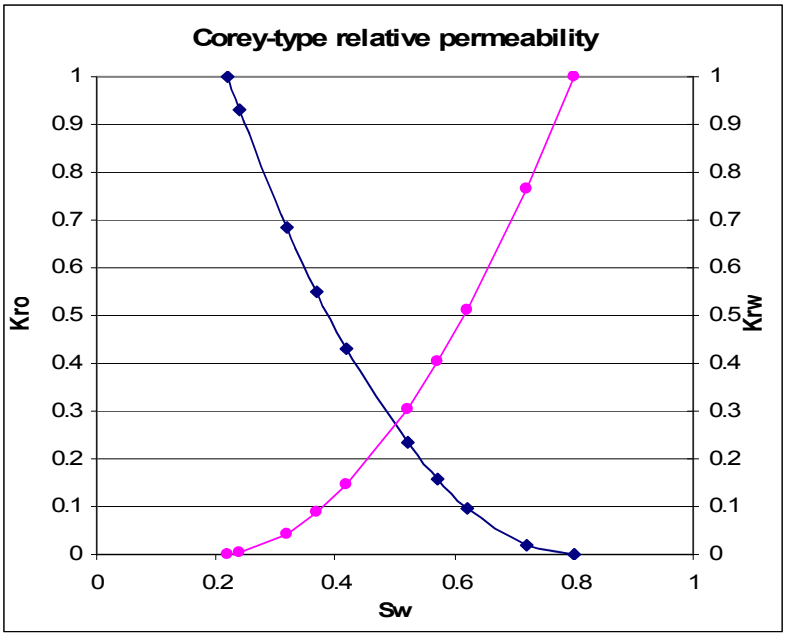

Figure 4.9 Corey-type relative permeability curves

Obtained values were used in Eclipse input file for all simulation runs.

4.3.2 Fractional flow calculations

In a waterflood in which there is no saturation gradient behind the waterflood front, there is no ambiguity about the value of water relative permeability to be used. However, in my research in which there is a saturation gradient behind the flood front, how can we select the appropriate value of water relative permeability?

Some of the early experimental results avoided that question by the use of flow models with miscible fluids in which there is no saturation gradient behind the injected fluid front. In 1955, Craig et al. presented the results of waterflood model in five-spot pattern. A variety of oil viscosities used to obtain a range of saturation gradients and it was found that if the water mobility was defined at the average water saturation behind the flood front at water breakthrough, the data on areal sweep versus mobility ratio would match those obtained by using miscible fluids. As a result of those studies, the water mobility is defined as that at the average water saturation in the water-contacted portion of the reservoir and this definition has been widely accepted.[3]

After obtaining relative permeabilities for oil and water, the fractional flow curves for each viscosity ratio μ_o/μ_w is to be found. Using the definition of fractional flow,

$$fw = \frac{1}{1+\frac{\mu_w}{k_{rw}}\frac{k_{ro}}{\mu_o}} \quad \text{,.....} \quad (4.4)$$

By substituting for k_{ro} and k_{rw} from **Eqs. 3.1** and **3.2**, we can build charts **(Fig. 4.10** through **Fig. 4.13)** that help us to obtain average water saturation behind flood front $\overline{S_w}$ for each corresponding μ_o/μ_w ratio.

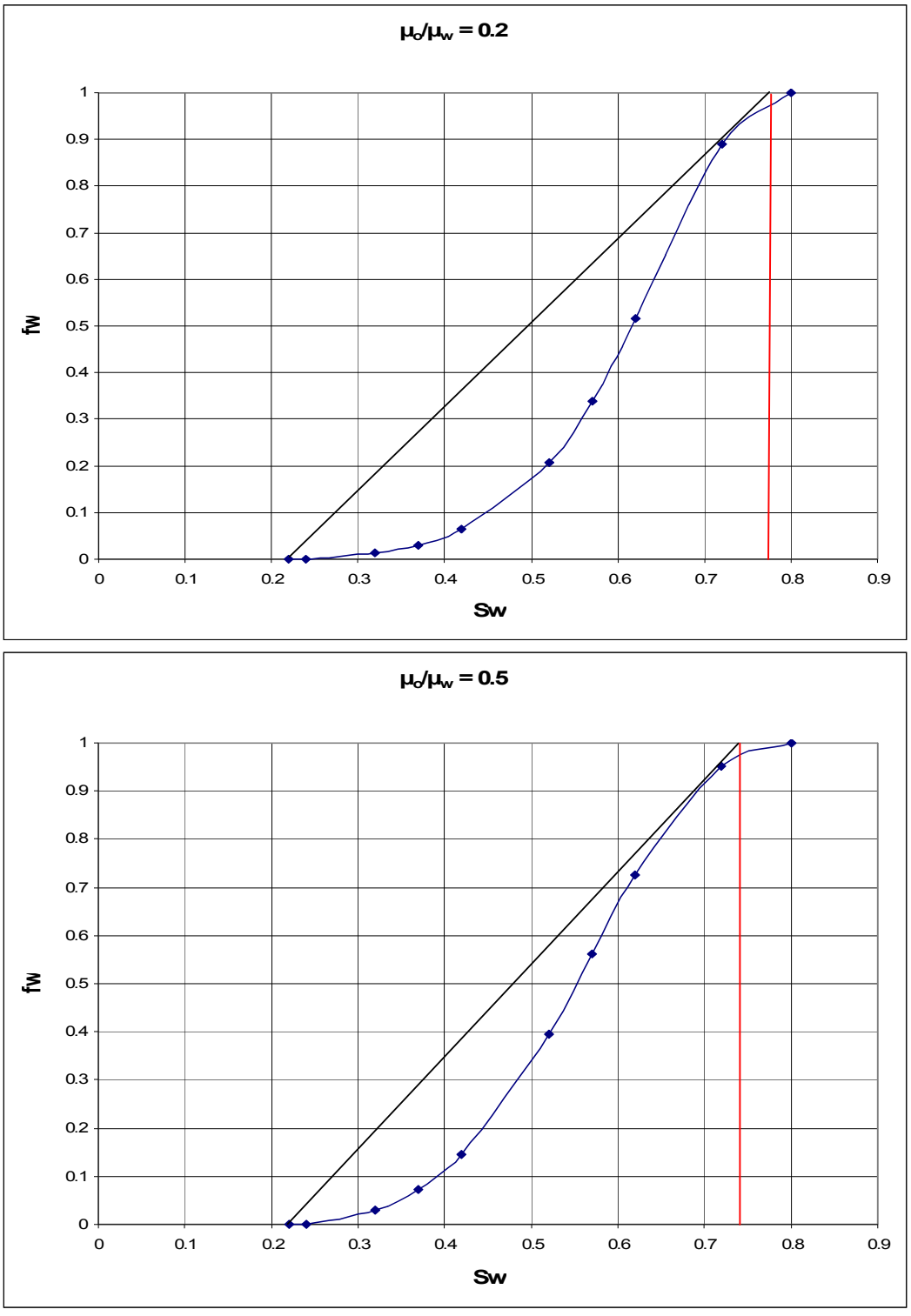

Figure 4.10 Fractional flow curves for μ_o/μ_w ratio equal 0.2 and 0.5

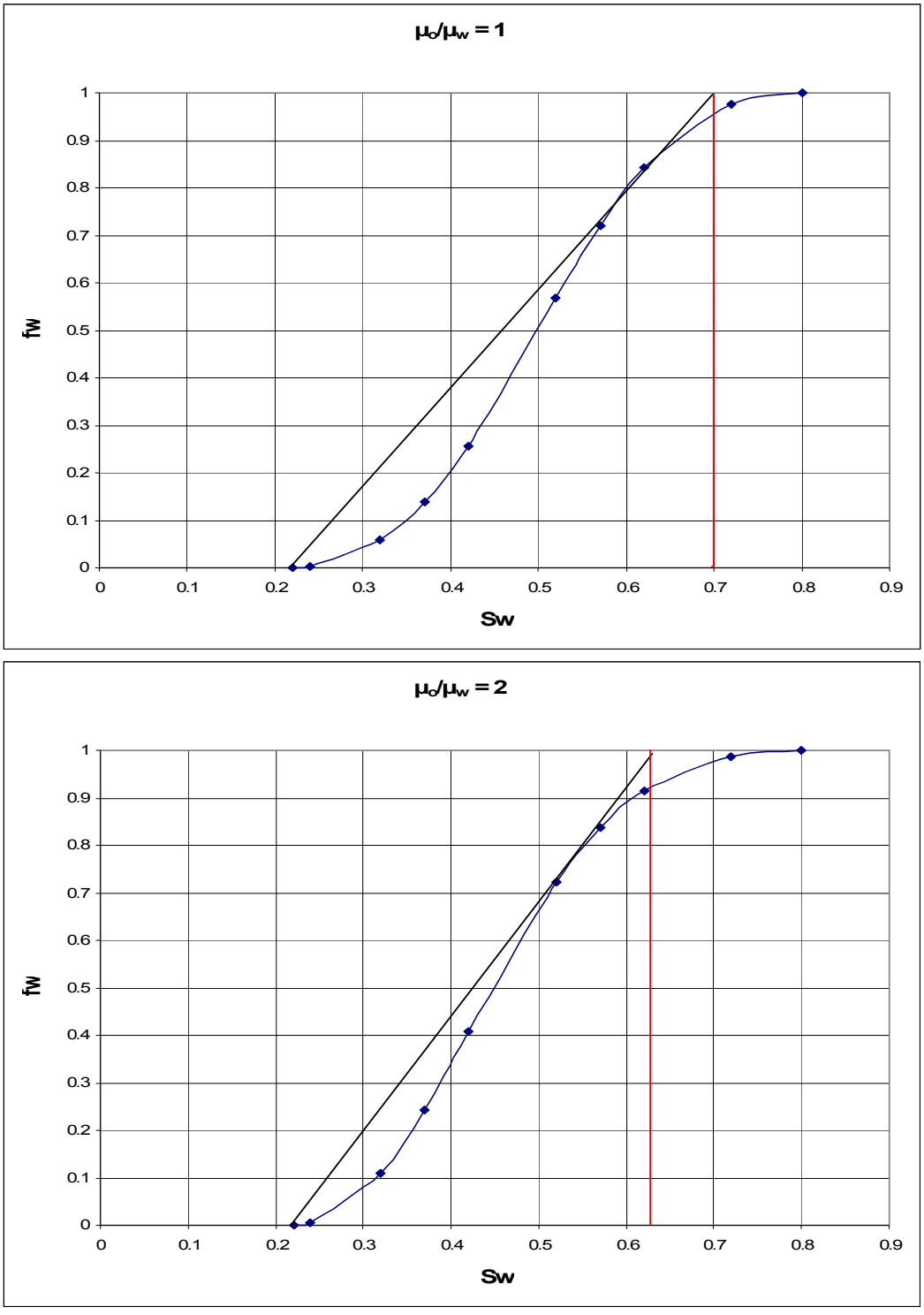

Figure 4.11 Fractional flow curves for μ_o/μ_w ratio equal 1 and 2

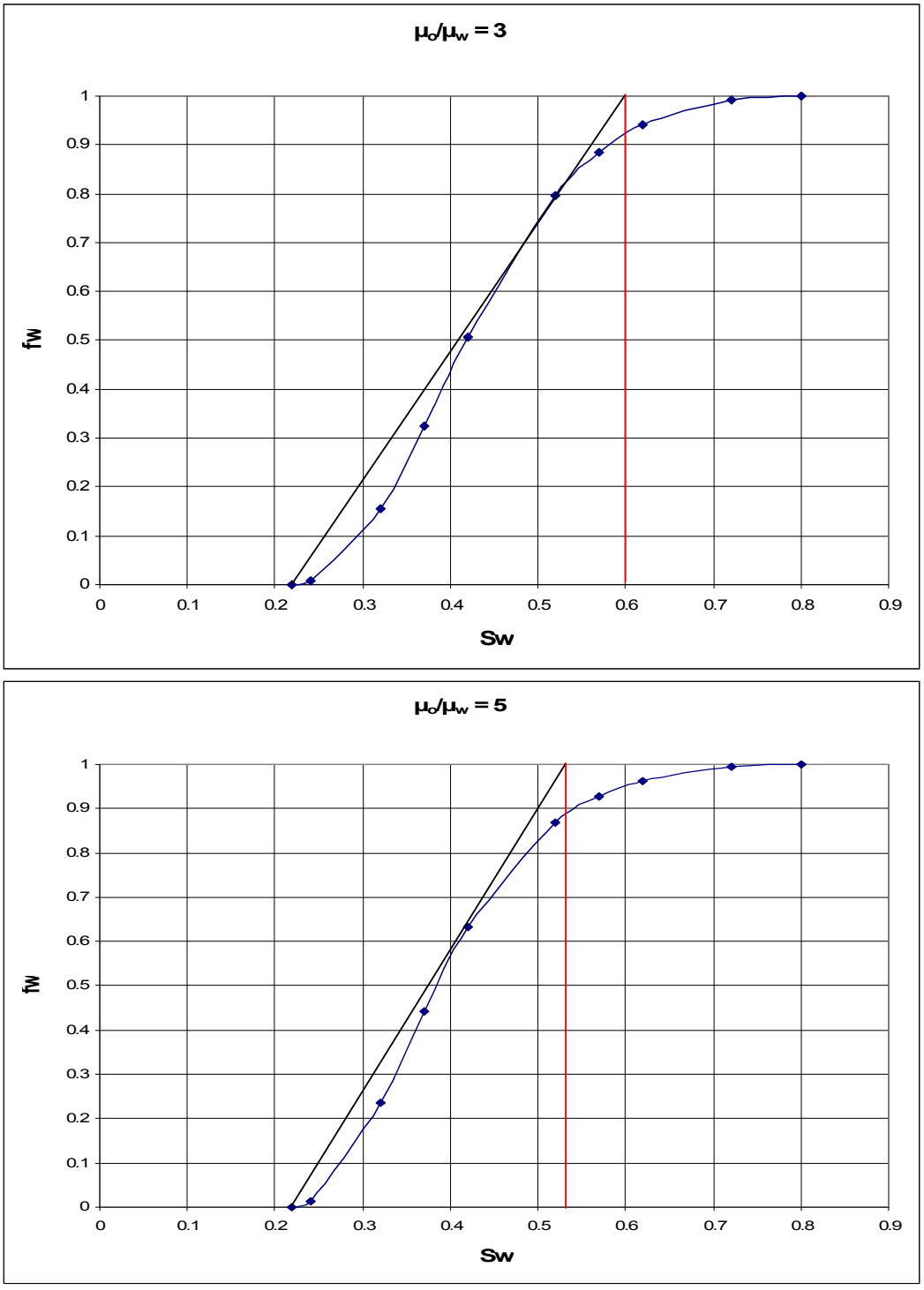

Figure 4.12 Fractional flow curves for μ_o/μ_w ratio equal 3 and 5

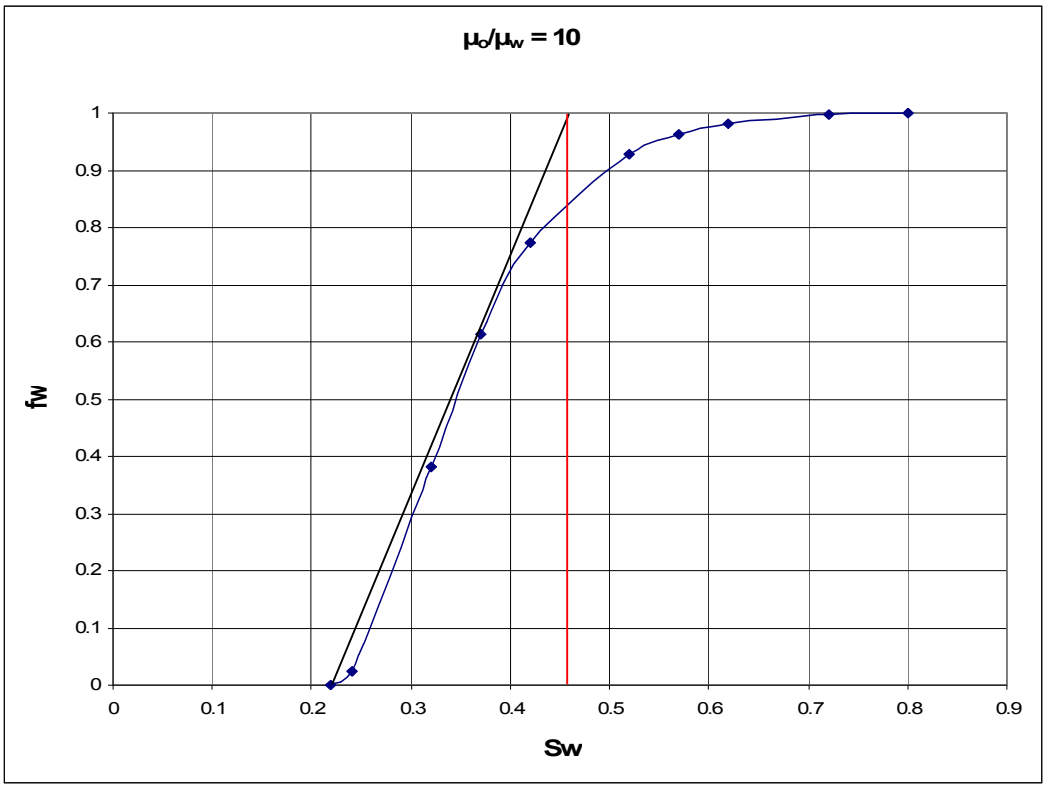

Figure 4.13 Fractional flow curve for μ_o/μ_w ratio equal 10

To find $\overline{S_w}$ value we needed to the know exact point of the intersection of the tangent of the fractional flow curve with the maximum water fraction that equals 1, then simply by drawing a line from that intersection to S_w scale we obtain the average water saturation behind the water front for each μ_o/μ_w case:

μ_o/μ_w =0.2; $\overline{S_w}$ = 0.77

μ_o/μ_w =0.5; $\overline{S_w}$ = 0.74

μ_o/μ_w =1; $\overline{S_w}$ = 0.7

μ_o/μ_w =2; $\overline{S_w}$ = 0.635

μ_o/μ_w =3; $\overline{S_w}$ = 0.6

μ_o/μ_w =5; $\overline{S_w}$ = 0.53

μ_o/μ_w =10; $\overline{S_w}$ = 0.45

4.3.3 Mobility ratio calculation

We will use these values to calculate the end point water relative permeability k_{rwe} for each viscosity ratio by applying **Eq. 4.2** and substituting S_w on the obtained $\overline{S_w}$ in **Eq. 4.3**. Then using **Eq. 1.2** we can estimate the mobility ratio *M*, calculated values presented in Table 4.1.

Table 4.1

μ_o/μ_w	$\overline{S_w}$	K_{rwe}	M
0.2	0.77	0.909	0.182
0.5	0.74	0.822	0.411
1	0.7	0.711	0.711
2	0.635	0.547	1.095
3	0.6	0.467	1.401
5	0.53	0.324	1.619
10	0.45	0.189	1.892

4.3.4 Breakthrough determination

In the following sections I presented calculations that correspond to a five-spot waterflood pattern with finest 60x30x1model, similar methodology can be used for all other models and patterns. Fractional flow at the producer versus displacing fluid injected obtained from the simulation output file (RSM) where f_w is water fraction at the producer and W_{iD} is dimensionless value of water injected at injector.

$$W_{iD} = \frac{0.000129 * W_i}{Ah\phi(1 - S_{wc} - S_{or})}, \quad \text{.....(4.5)}$$

Where W_i is cumulative water injected at certain time, A is for grid block area which in our case equal 40 acres, h is 20 ft. and φ equal 0.3 for total porosity.

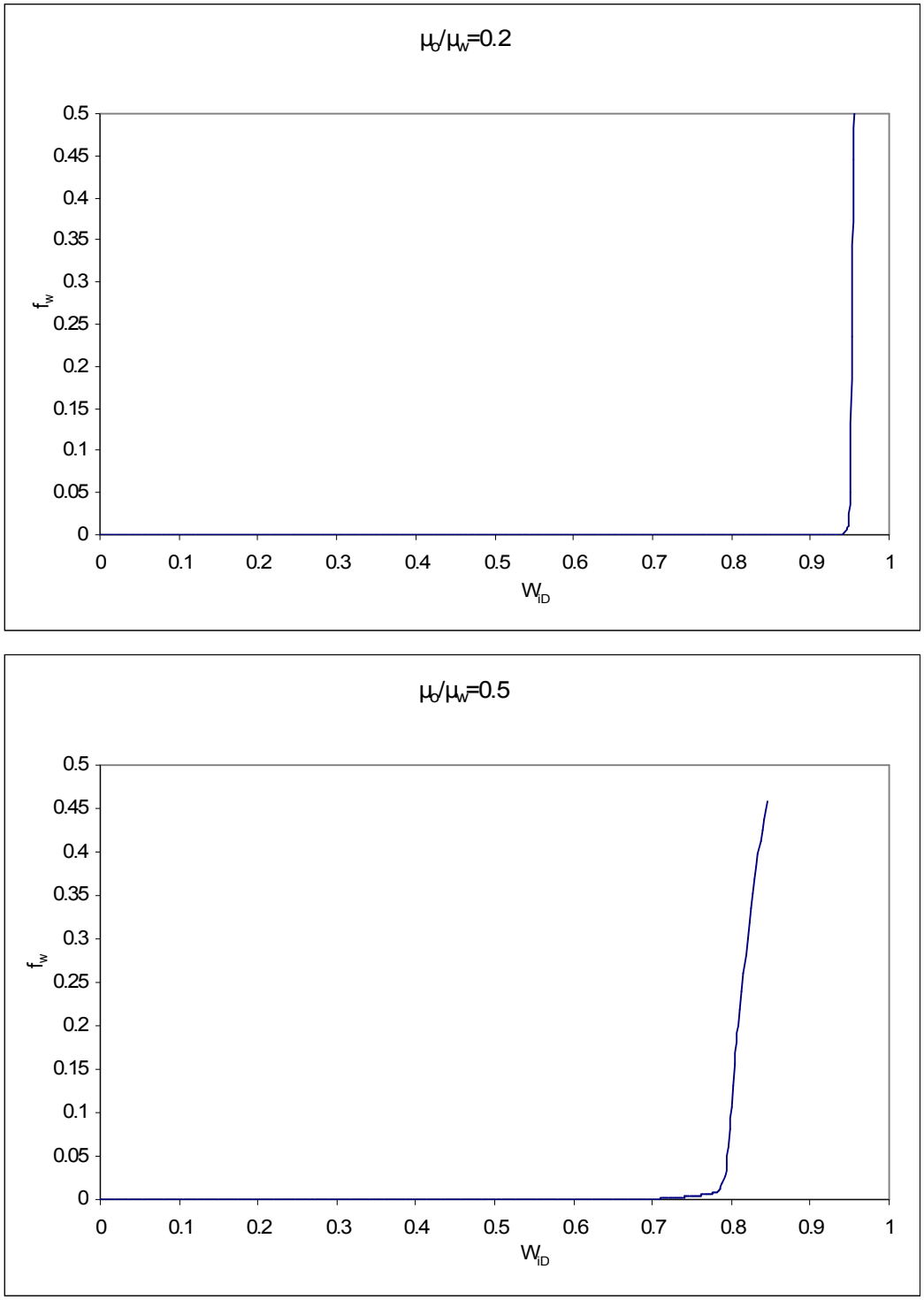

Figure 4.14 Fractional flow f_w versus W_{iD} for viscosity ratios μ_o/μ_w equal 0.2 and 0.5

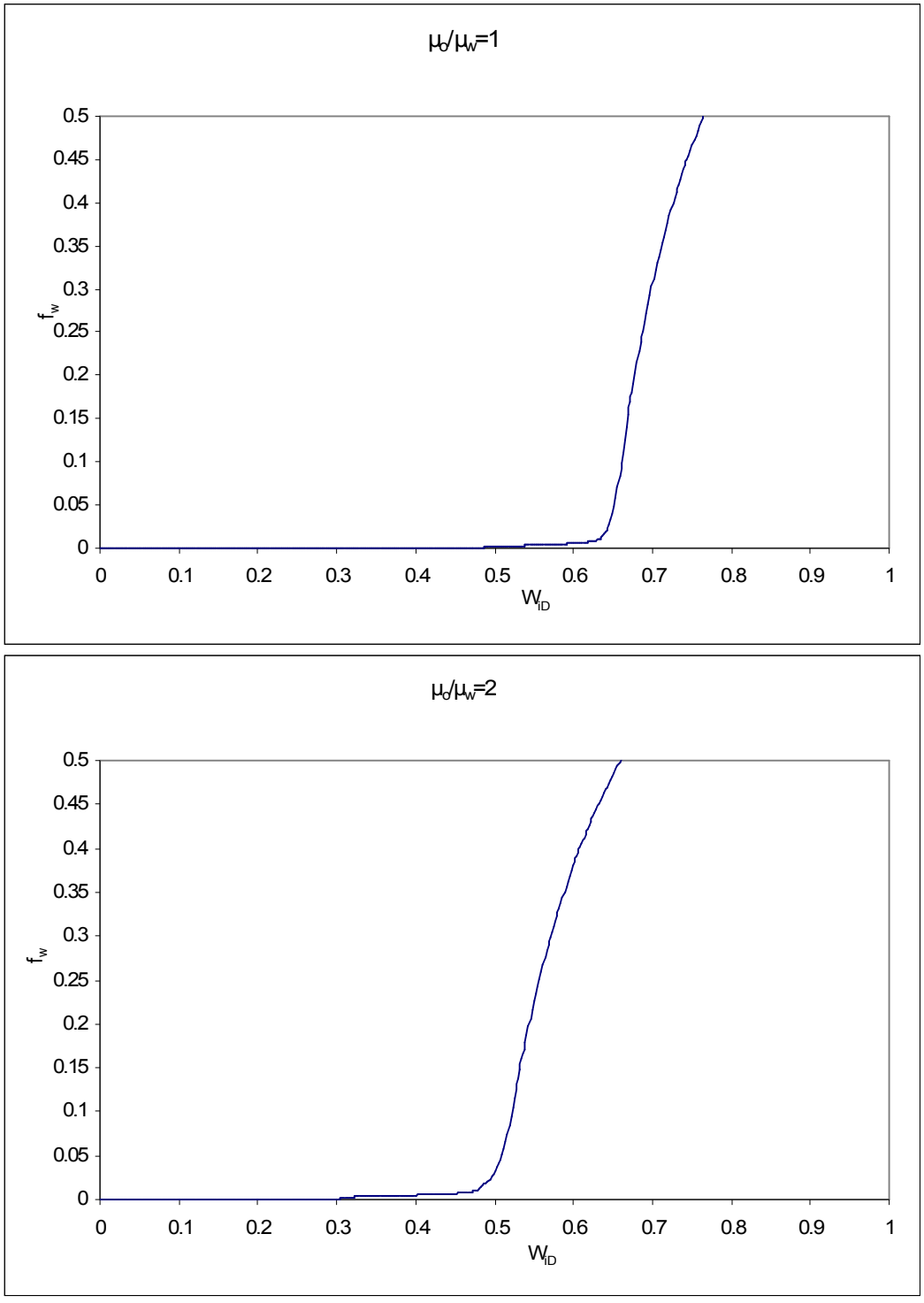

Figure 4.15 Fractional flow f_w versus W_{iD} for viscosity ratios μ_o/μ_w equal 1 and 2

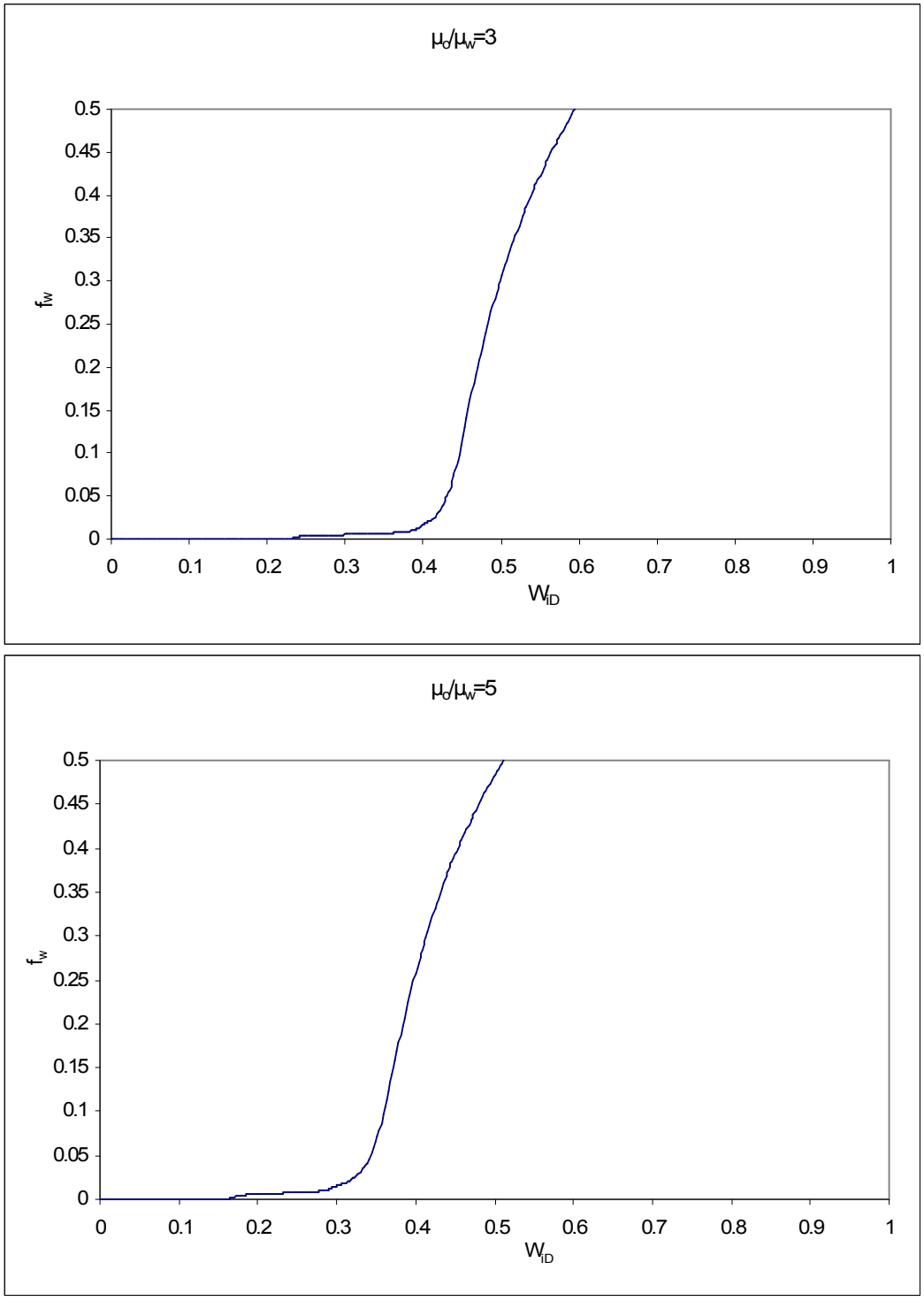

Figure 4.16 Fractional flow f_w versus W_{iD} for viscosity ratios μ_o/μ_w equal 3 and 5

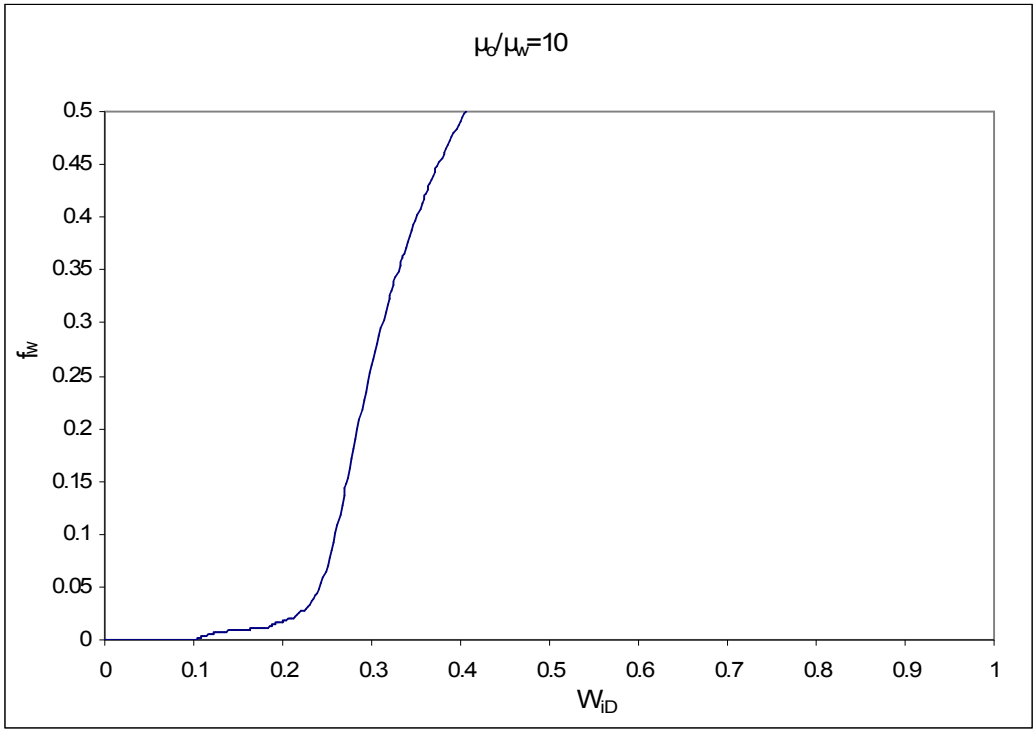

Figure 4.17 Fractional flow f_w versus W_{iD} for viscosity ratio μ_o/μ_w equal 10

Due to numerical dispersion of simulation, injected fluid breaks through earlier at the producer than it should. The fractional flow versus W_{iD} plots shown in **Fig. 4.14** through **Fig. 4.17** illustrate the early breakthrough caused by numerical dispersion.

To correct for numerical dispersion in breakthrough times and approximate the breakthrough time more accurately, we use fractional flow data after breakthrough and extrapolate back to breakthrough time. A third order polynomial is used for this method except for case when μ_o/μ_w is equal 0.2 (second order used to get smaller divergence). Microsoft Excel build-in trend line function were used obtain the polynomial fits presented in charts in **Fig. 4.18** through **Fig. 4.21**.

$$W_i = af_w^3+bf_w^2+cf_w+d, \quad (4.6)$$

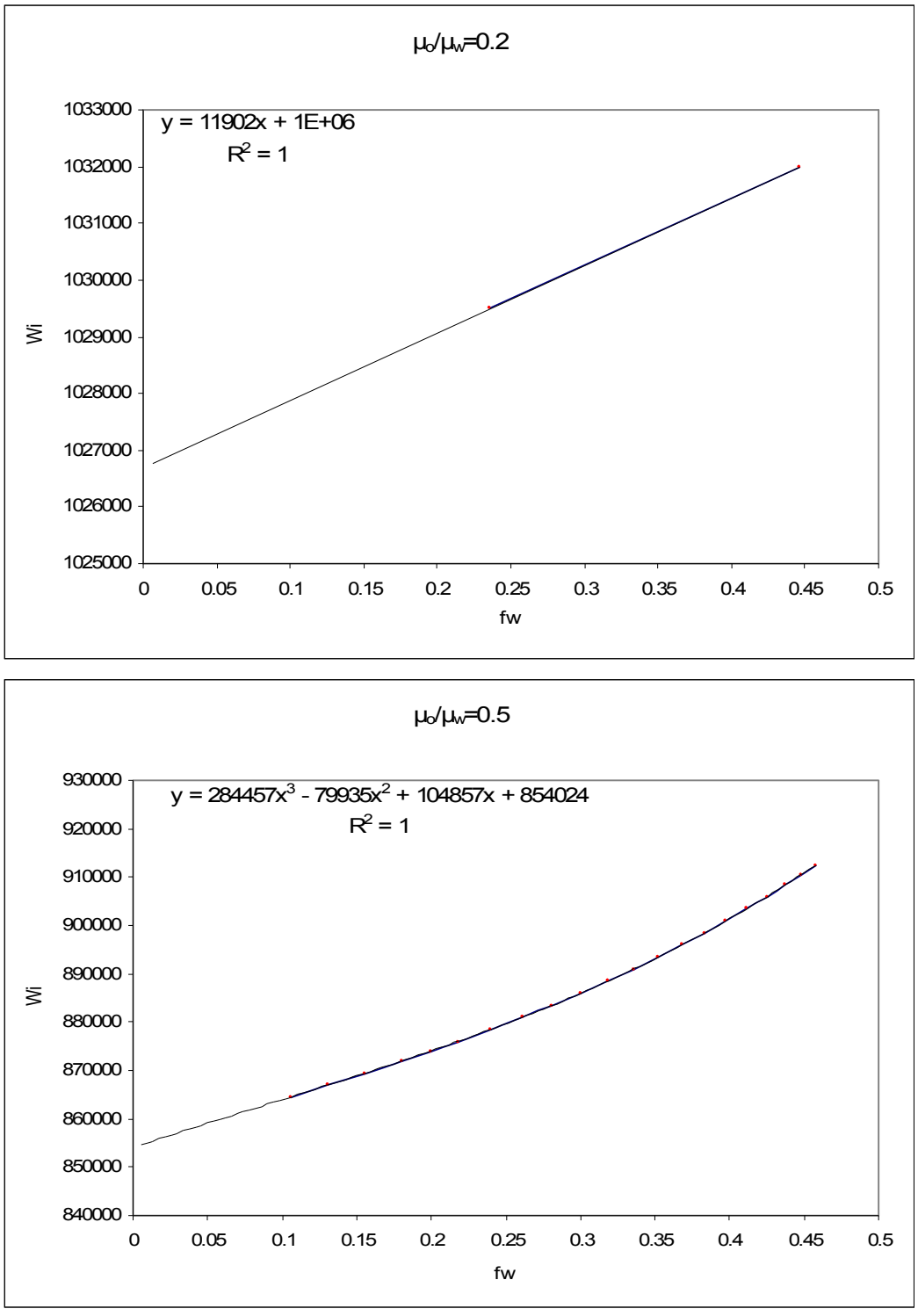

Figure 4.18 W_i versus fractional flow f_w for viscosity ratios μ_o/μ_w equal 0.2 and 0.5

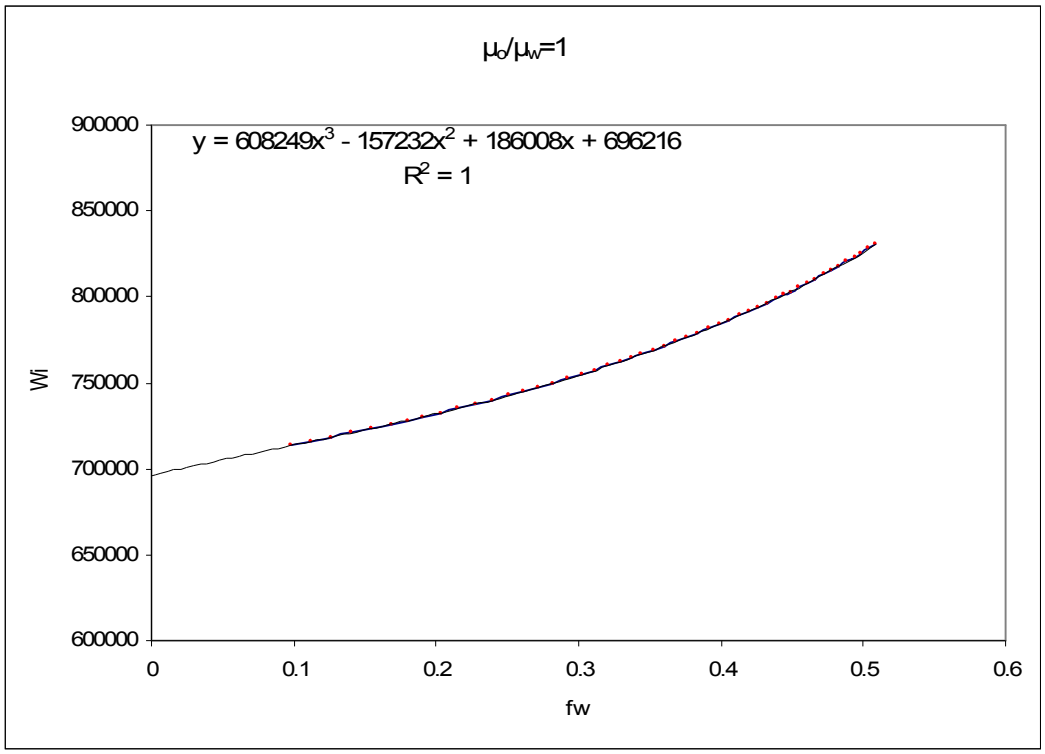

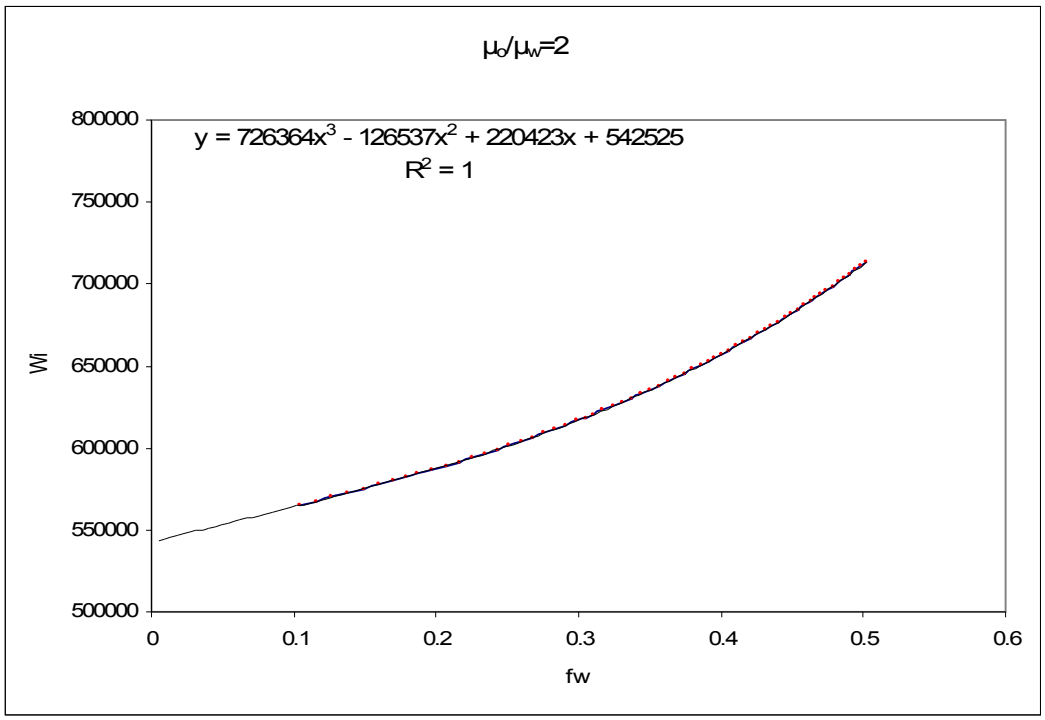

Figure 4.19 W_i versus fractional flow f_w for viscosity ratios μ_o/μ_w equal 1 and 2

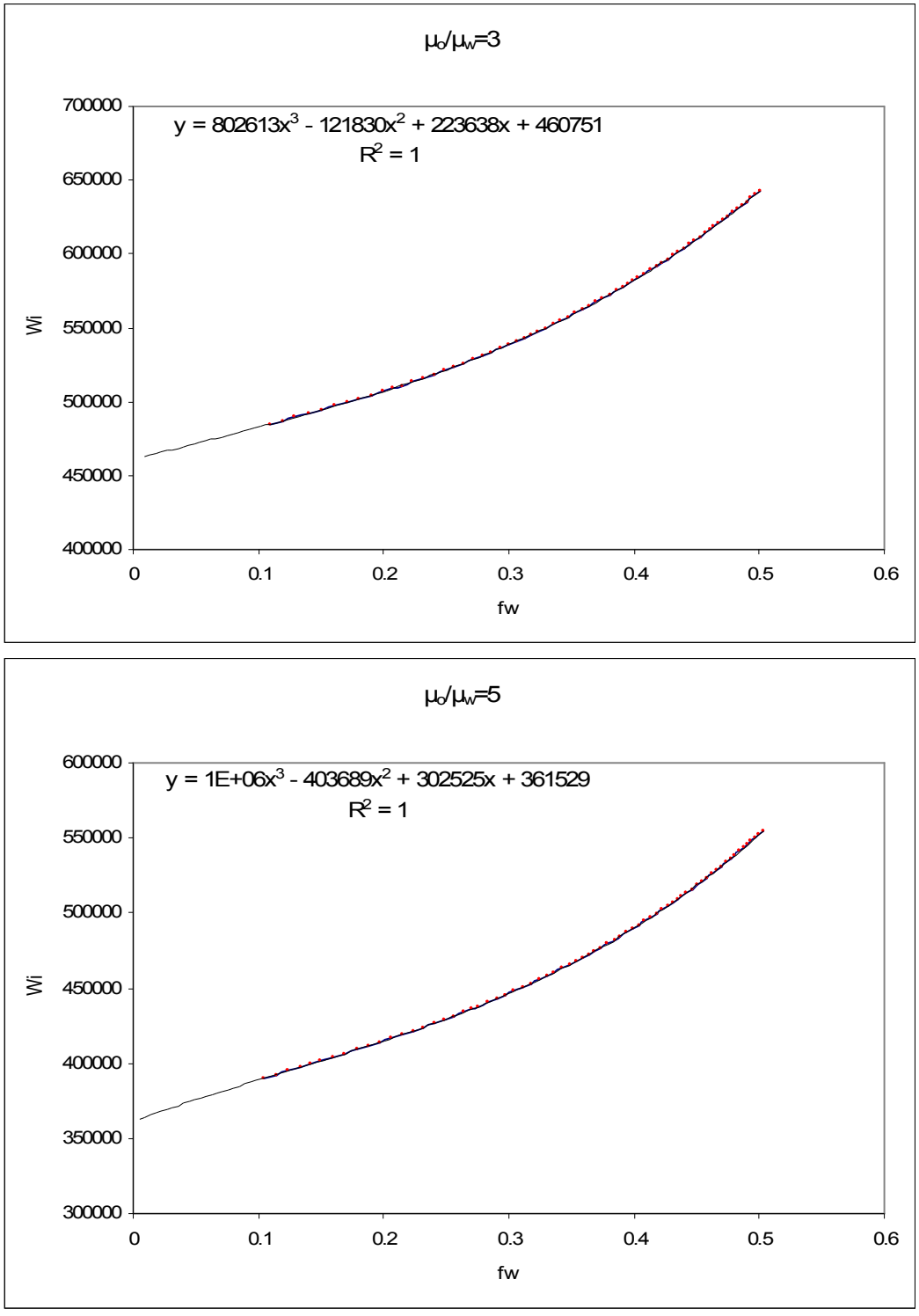

Figure 4.20 W_i versus fractional flow f_w for viscosity ratios μ_o/μ_w equal 3 and 5

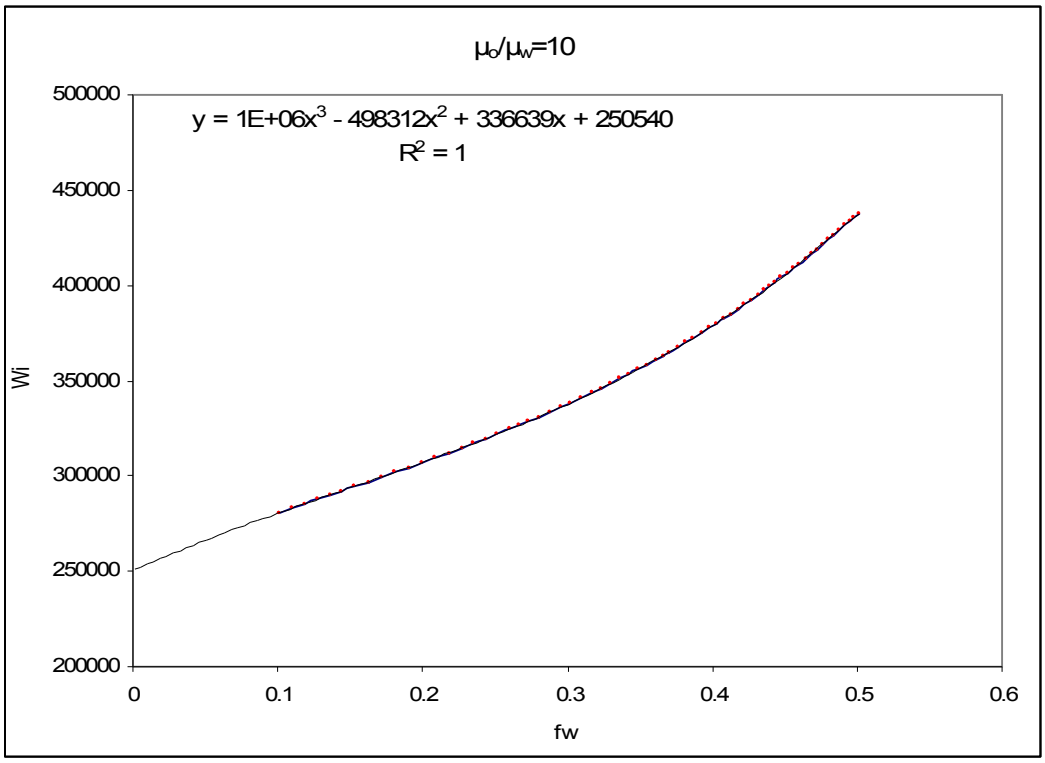

Figure 4.21 W_i versus fractional flow f_w for viscosity ratio μ_o/μ_w equal 10

From **Eq. 3.6** we use "d" coefficient as a value of cumulative water injected at breakthrough because with this value polynomial equations intersect W_i scale, that tells us very accurately when water fraction f_w begin to appear (breakthrough). Then, simply using **Eq. 1.5** and applying obtained W_i values we estimate areal sweep efficiency for each defined mobility ratio.

CHAPTER V
SIMULATION RESULTS

Finally, I made simulation runs and determined areal sweep efficiencies at breakthrough for other grid block dimensions and staggered line drive patterns with various aspect ratios. These are described below.

Fig. 5.1 graphically presents simulated results for 40x20x1 model and experimental results obtained in different time by different investigators. It shows very good agreement between these models, however for mobility ratios greater than 1 (M>1) we can notice that simulation areal sweep efficiency begins to decrease much faster than it is for experiments.

For 60x30x1 grid model illustrated in comparison with experimental results in **Fig. 5.2,** there is greater deviation in simulation areal sweep efficiency results than it is for 40x20x1 model, but considering areal sweep efficiency values for M>1 we see much better alignment with experimental results. This advantage lets us use a larger range of mobility ratios for pattern behavior investigation.

Fig. 5.3 represents all simulation results performed for the five spot pattern, this will help us to better understand the effect of grid block number on simulation results. In this figure, I also presented simulation results for 20x10x1 and 200x100x1 models. From the chart it is easy noticeable that 20x10x1 model has worse alignment with experiments as well as performance for unfavorable mobility ratios (M>1), this leads us to eliminate this model from further study of staggered line drive patterns behavior. Additional 200x100x1 grid block model used to better represent the effect of grid block number on simulation results and its reliability.

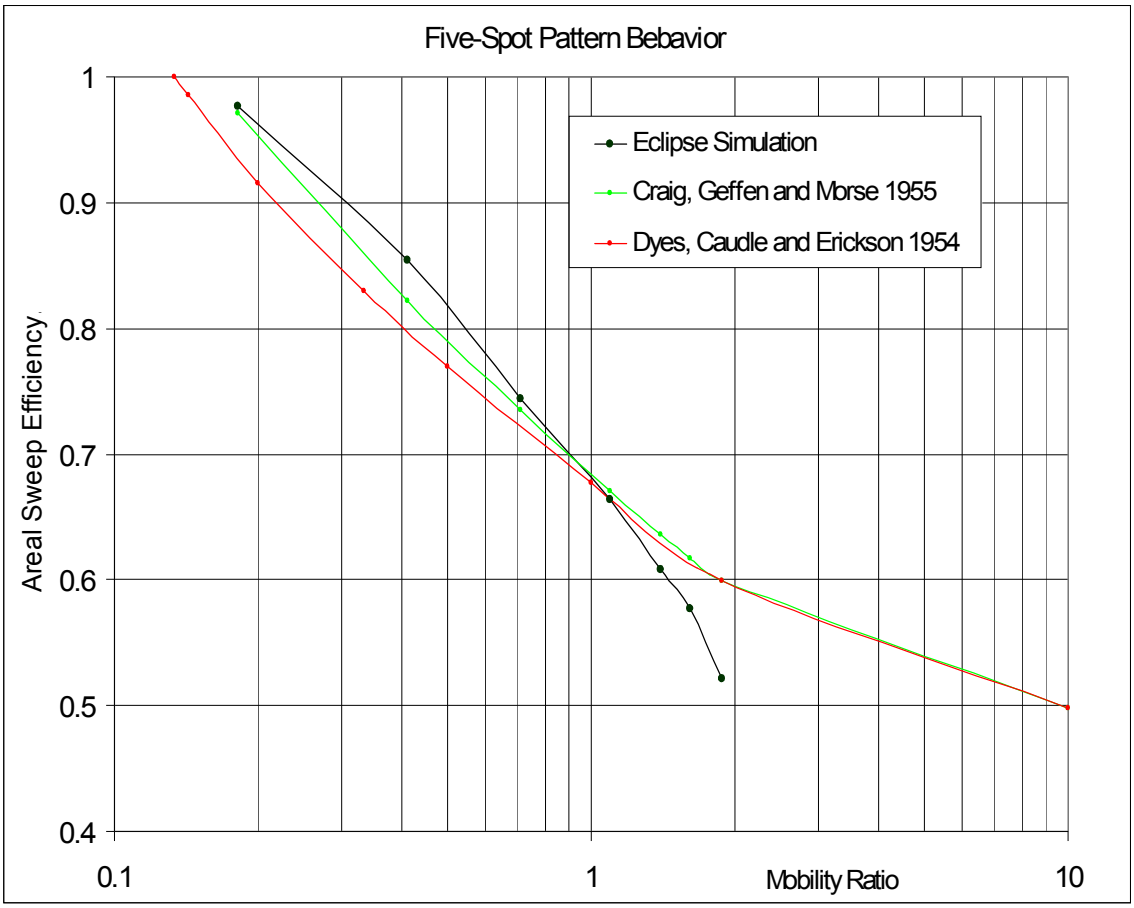

Figure 5.1 Comparison of Eclipse simulation results for 40x20x1 model with experimental values in five-spot waterflood pattern

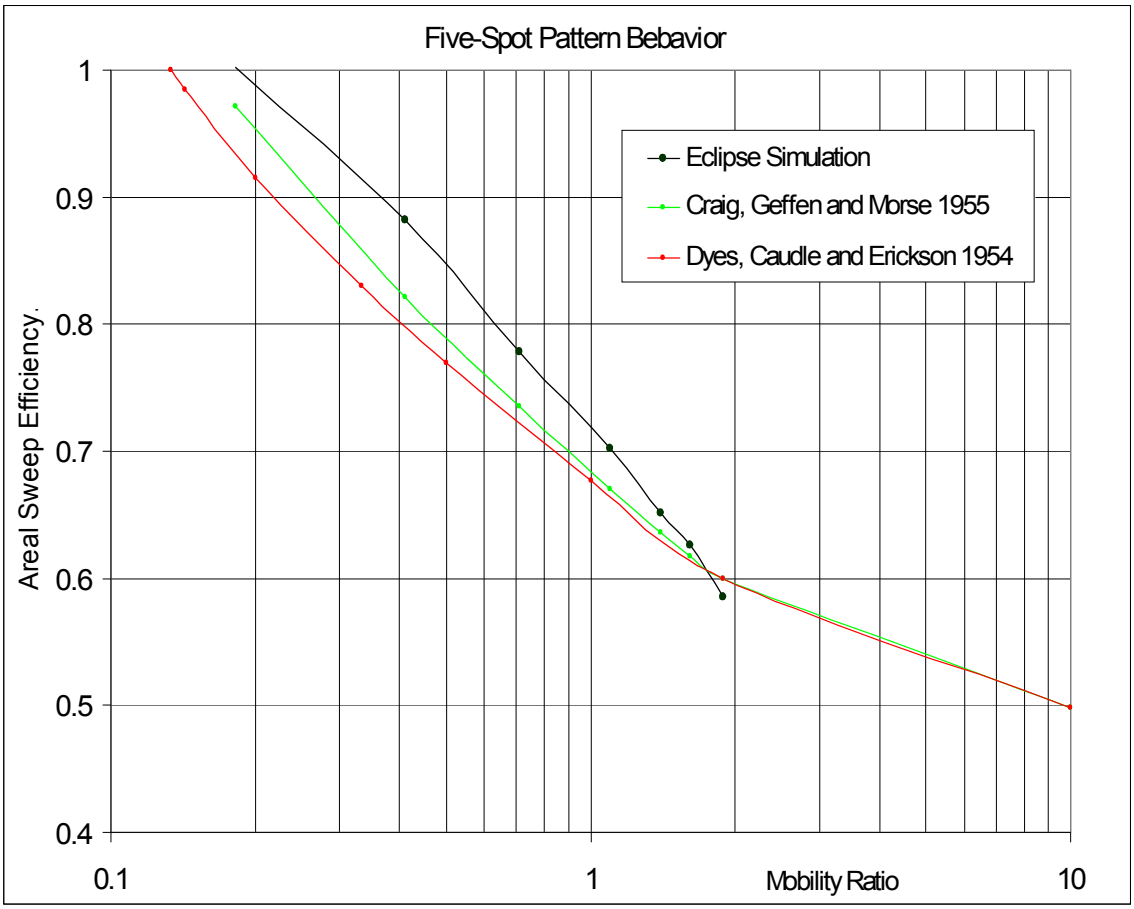

Figure 5.2 Comparison of Eclipse simulation results for 60x30x1 model with experimental values in five-spot waterflood pattern

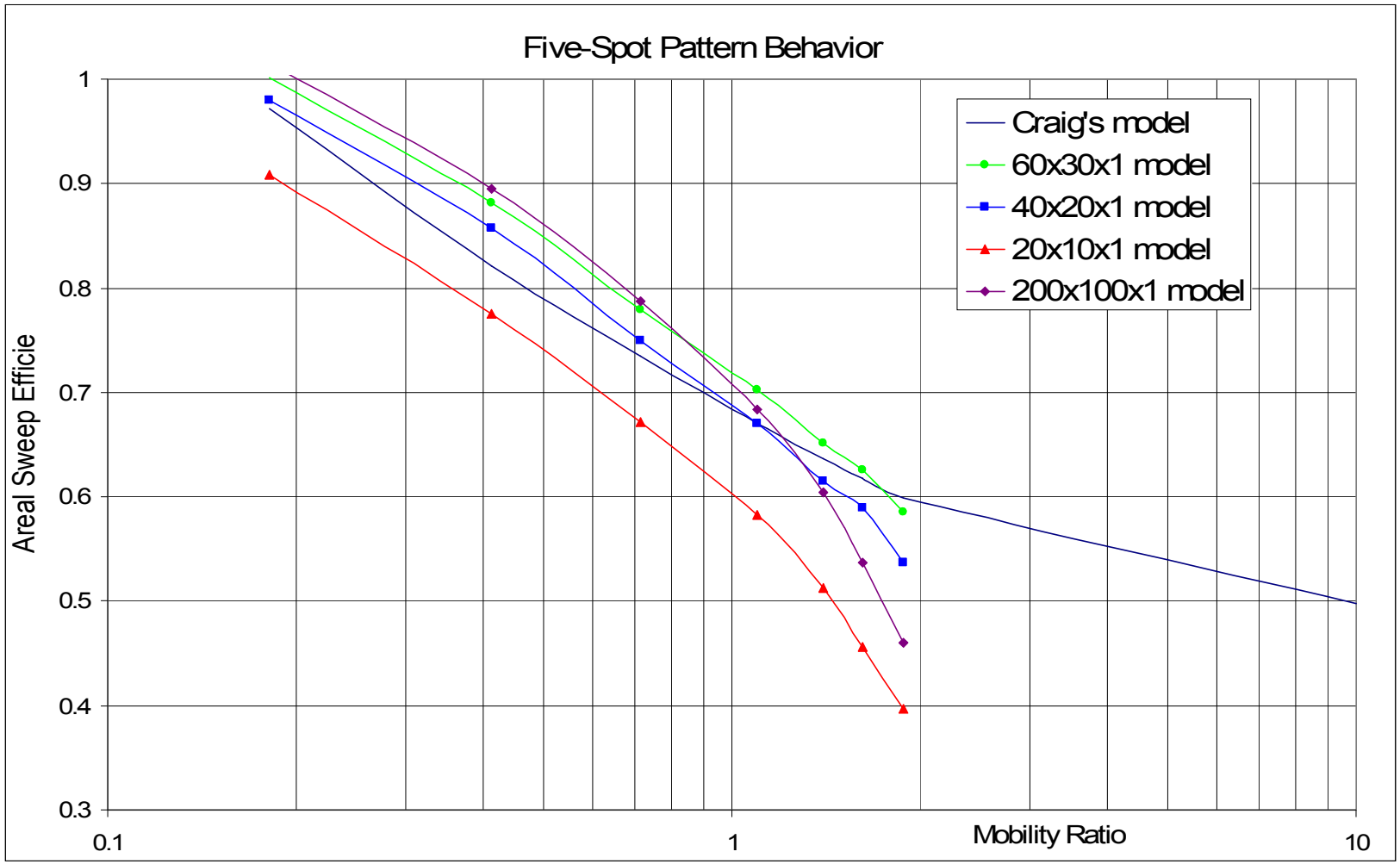

Figure 5.3 Illustration and comparison of five-spot pattern behavior for different grid models with Craig model

Figure 5.4 Comparison of 40x20x1 staggered line drive patterns simulation results for different aspect ratios (d/a) with Dyes experimental values for d/a=1

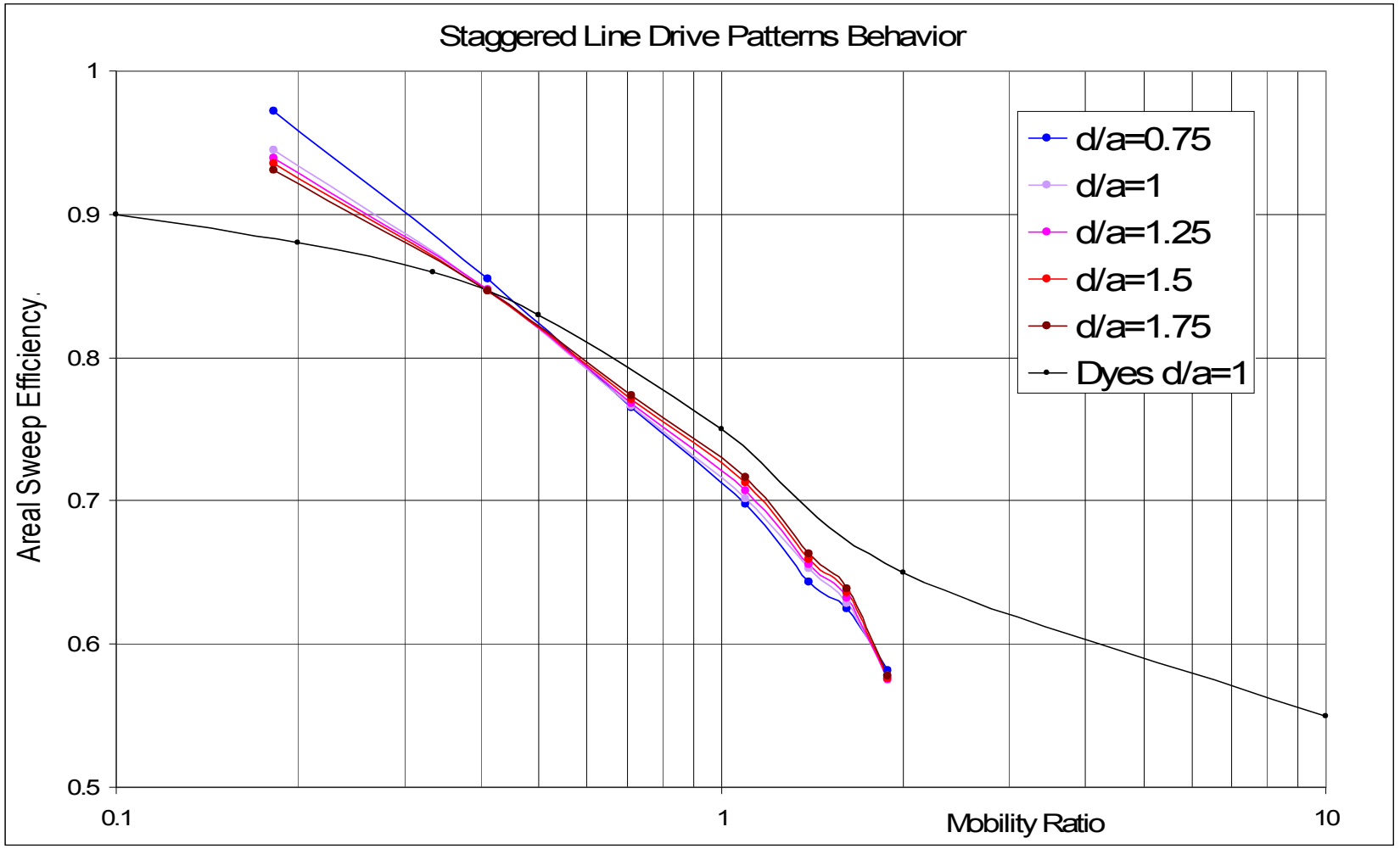

Figure 5.5 Comparison of 60x30x1 staggered line drive patterns simulation results for different aspect ratios (d/a) with Dyes experimental values for d/a=1

Fig. 5.4 shows staggered line drive pattern performance for different aspect ratios performed in 40x20x1 simulation model. Results compared against the Dyes experimental values for aspect ratio $d/a = 1$. We can see poor agreement between simulation and experimental values for areal sweep efficiencies may caused by relatively small grid block number (40x20x1).

Next chart (**Fig. 5.5**) presents the same results only for 60x30x1 grid block model. Here we can notice large improvement in terms of alignment. Best agreement between simulation results and experimental occurs approximately in 0.4-0.6 mobility ratio range where the affect of aspect ratio on areal sweep is negligible.

In the following graphs (**Fig. 5.6** and **Fig. 5.7**) I showed the obtained results in representation of flood efficiencies for unit mobility ratio ($M = 1$), where we study the effect of aspect ratio (d/a) on pattern performance. Results of two models 40x20x1 and 60x30x1in each chart compared with experimental results obtained by different investigators. After comparing the simulation results of the first model (40x20x1) with Muskat's values we can set the deviation range that vary from 0.08 to 0.16 of areal sweep efficiency, for second (60x30x1) it is from 0.04 to 0.08.

Again, for 40x20x1 model it is clear that agreement with experiments is worse than it is for another (60x30x1) not only considering wider deviation range but also because of reverse curve's trend i.e. areal sweep efficiency decrease with increase of aspect ratio.

Thus after summarizing the facts concluded from presented results, the simulation model that gives the most satisfactory match with experimental data is the 60x30x1 model.

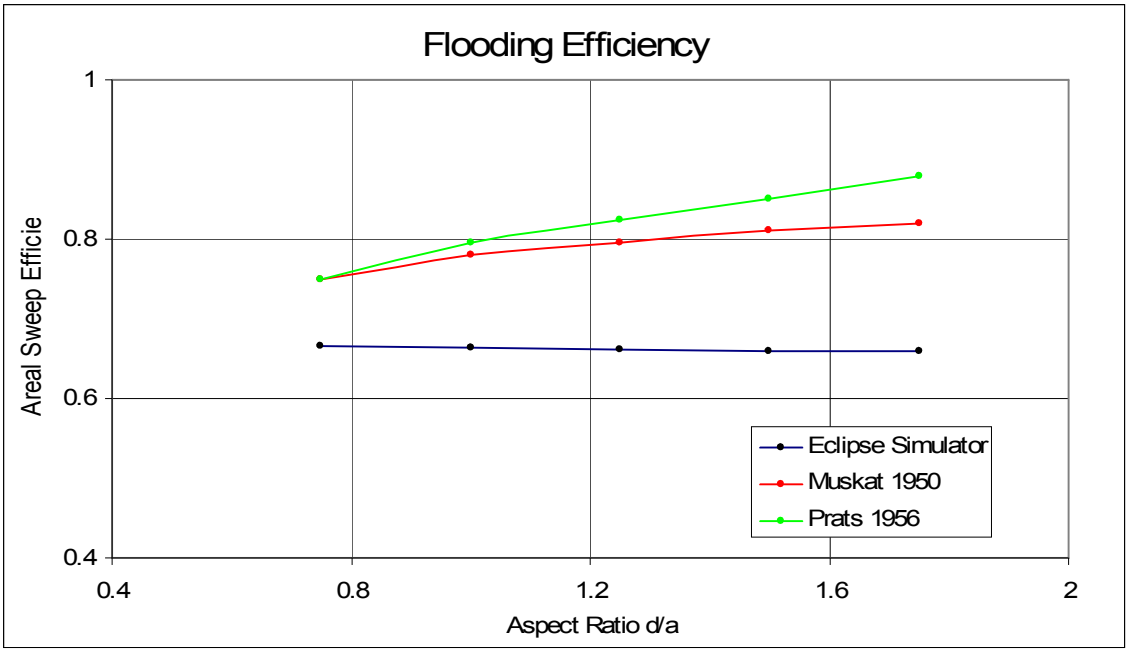

Figure 5.6 Comparison of 40x20x1 model's flood efficiency for unit mobility ratio (M=1)

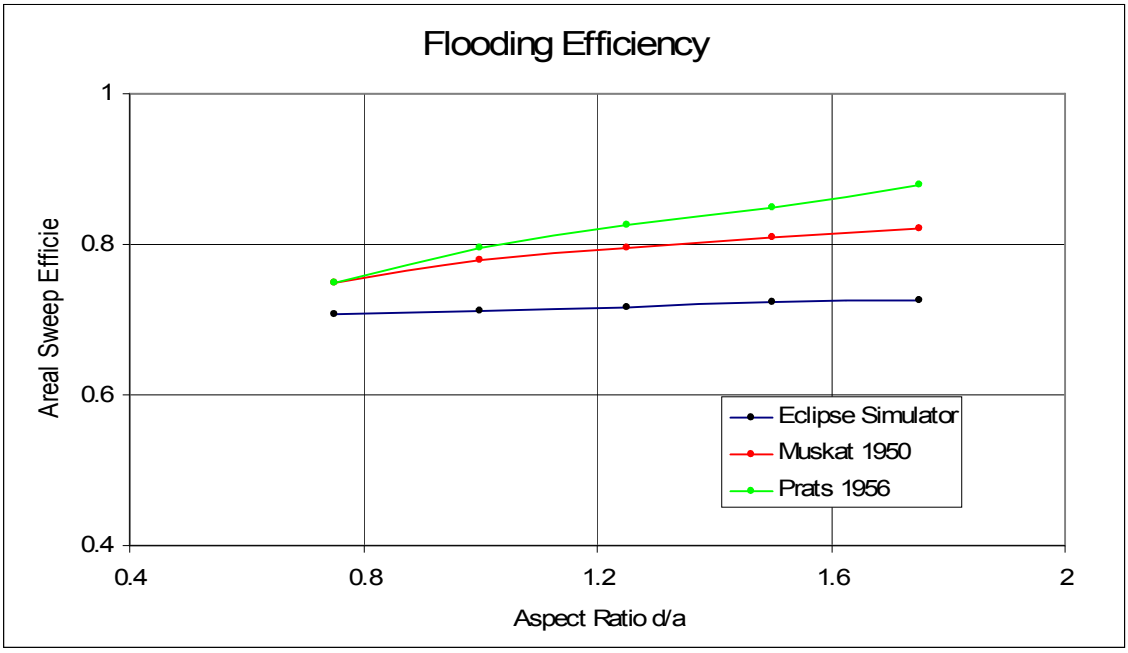

Figure 5.7 Comparison of 60x30x1 model's flood efficiency for unit mobility ratio (M=1)

CHAPTER VI
SUMMARY, CONCLUSIONS AND RECOMMENDATIONS

6.1 Summary

A simulation study has been performed with the main objective of determining the areal sweep efficiency at breakthrough for waterflood staggered line drive as a function of the Craig mobility ratio for a range of aspect ratios. The two-dimensional simulation model represents 1/8 of a 40-acre pattern unit with a reservoir thickness of 20 ft. Simulation runs using a number of Cartesian grid models were made to determine the optimum grid model. The Cartesian models tested were 20x10x1, 40x20x1, 60x30x1 and 200x100x1. The simulation results of areal sweep efficiency versus mobility ratio were compared against available experimental data for 5-spot pattern and staggered line drive with aspect ratio of 1. The simulation model that gave the most satisfactory match with experimental data was the 60x30x1 model and therefore was selected for detailed study.

6.2 Conclusions

The main conclusion of the simulation study may be summarized as follows:

1. For staggered line drive patterns, simulation results are in very satisfactory agreement with experimental data for water-oil mobility ratio in the range, 0.4-0.6, where the affect of staggered line drive aspect ratio on areal sweep at breakthrough is not significant. For mobility ratio above 0.6 and aspect ratio of 1, the areal sweep efficiency at breakthrough shows a slightly higher trend compared to simulation data (for example, 0.72 versus 0.75 at mobility ratio of 1. For mobility ratio less than 0.4, the simulated areal sweep efficiency is slightly higher than the experimental data (for example, 0.93 versus 0.88 at mobility ratio of 0.2).
2. Areal sweep efficiency decreases with an increase in mobility ratio – in line with experimental data - for all aspect ratios. These results clearly indicate that water-oil mobility ratio controls the displacement of oil by water at the pore level.
3. Areal sweep efficiency increases with an increase in aspect ratio (for mobility ratios greater than 0.5) – in line with experimental data. The results underscore the fact that

the aspect ratio in a staggered line drive controls the displacement of oil by water at the macro level.

4. A major problem encountered during the study is the determination of breakthrough time. This problem has been reported by others doing similar type of research. The main cause of the problem is probably numerical dispersion, although just increasing the number of grid blocks in the model does not seem to completely eliminate the problem.

6.3 Recommendations

The following recommendations are suggested for future research:

1. The simulation study indicates the importance of choosing an optimal number of grid blocks in a simulation model, so as to obtain minimum dispersion yet not to have a too large a model that will take too long to run.

2. For future studies, it is suggested to limit the mobility ratio range to about 0.2 to 1.5, to avoid discrepancy (stemming from numerical dispersion) with experimental results.

3. It is recommended to investigate the possibility of minimizing or eliminating the numerical dispersion problem by, for instance, the use of streamline simulation.

NOMENCLATURE

A_S area swept, sqft

A_T total area of the pattern, sqft

a distance between like wells (injection or production) in a row, ft

d distance between adjacent rows of injection and production wells, ft

E_A areal sweep efficiency

f_w fractional flow of water

h bed thickness, ft

k permeability, mD

k_{ro} relative permeability of oil

k_{rw} relative permeability of water

M mobility ratio

ϕ porosity

μ viscosity,cp

W_i volume of displacing phase injected,

REFERENCES

Brigham, William E., Kovscek, Anthony R., Wang, Y. 1998. A Study of the Effect of Mobility Ratios on Pattern Displacement Behavior and Streamline to infer Permeability Fields Permeability Media. MS thesis, SUPRI-A.

Craig, F. F. Jr. 1971. *The Reservoir Engineering Aspect of Water Flooding*. SPE Monograph, Vol. 3.

Dyes, A.B., Caudle B.H., and Erickson R.A.1954. Oil Production after Breakthrough – as Influenced by Mobility Ratio. *Petroleum Trans.* AIME, **201**: 27-32.

Morel-Seytoux, H.J., 1966. Unit Mobility Ratio Displacement Calculations for Pattern Floods in Homogeneous Medium. *SPE*, **6**: 217-227.

Peaceman, D.W. 1977. *Fundamentals of Numerical Reservoir Simulation*. New York: Elsevier Scientific Publishing Co.

Pitts, Gerald N., Crawford, Paul B. 1971. Simulating Large Flow Networks in Underground Media. New York, ACM.

Prats, M. 1956. The Breakthrough Sweep Efficiency of the Staggered Line Drive. *Trans.* AIME, **207**: 67-68.

Willhite, G.P. 1986. *Waterflooding*. SPE Textbook Series Vol. 3. Richardson, Texas, SPE.

APPENDIX

ECLIPSE RUN FILE EXAMPLE

```
RUNSPEC

TITLE
 FIVE-SPOT FOR 20 by 10 GRID BLOCK

DIMENS
  20   10    1  /

OIL

WATER

FIELD

TABDIMS
   1    1   20    2    1   20 /

WELLDIMS
   2    1    1    2 /

START
  1 'JAN' 1983  /

NSTACK
   8 /

FMTOUT

FMTIN

UNIFOUTS

GRID    ============================================================

     -- DX ----------
BOX
01 01 01 10 01 1 /
DX
10*24.00004769
/
BOX
02 02 01 10 01 1 /
DX
10*48.00009538
/
BOX
03 03 01 10 01 1 /
DX
10*72.00014306
/
BOX
```

```
04 04 01 10 01 1 /
DX
10*96.00019075
/
BOX
05 05 01 10 01 1 /
DX
10*120.0002384
/
BOX
06 06 01 10 01 1 /
DX
10*144.0002861
/
BOX
07 07 01 10 01 1 /
DX
10*168.0003338
/
BOX
08 08 01 10 01 1 /
DX
10*192.0003815
/
BOX
09 09 01 10 01 1 /
DX
10*216.0004292
/
BOX
10 10 01 10 01 1 /
DX
10*240.0004769
/
BOX
11 11 01 10 01 1 /
DX
10*240.0004769
/
BOX
12 12 01 10 01 1 /
DX
10*216.0004292
/
BOX
13 13 01 10 01 1 /
DX
10*192.0003815
/
BOX
14 14 01 10 01 1 /
DX
10*168.0003338
/
BOX
15 15 01 10 01 1 /
```

```
DX
10*144.0002861
/
BOX
16 16 01 10 01 1 /
DX
10*120.0002384
/
BOX
17 17 01 10 01 1 /
DX
10*96.00019075
/
BOX
18 18 01 10 01 1 /
DX
10*72.00014306
/
BOX
19 19 01 10 01 1 /
DX
10*48.00009538
/
BOX
20 20 01 10 01 1 /
DX
10*24.00004769
/
ENDBOX

-- DY ========================
BOX
01 20 01 01 01 1 /
DY
20*24.00004769
/
BOX
01 20 02 02 01 1 /
DY
20*48.00009538
/
BOX
01 20 03 03 01 1 /
DY
20*72.00014306
/
BOX
01 20 04 04 01 1 /
DY
20*96.00019075
/
BOX
01 20 05 05 01 1 /
DY
20*120.0002384
/
```

```
BOX
01 20 06 06 01 1 /
DY
20*144.0002861
/
BOX
01 20 07 07 01 1 /
DY
20*168.0003338
/
BOX
01 20 08 08 01 1 /
DY
20*192.0003815
/
BOX
01 20 09 09 01 1 /
DY
20*216.0004292
/
BOX
01 20 10 10 01 1 /
DY
20*240.0004769
/
ENDBOX

poro
  01*0.0375 18*0.15 01*0.0375
01*0 01*0.15 16*0.3 01*0.15 01*0
02*0 01*0.15 14*0.3 01*0.15 02*0
03*0 01*0.15 12*0.3 01*0.15 03*0
04*0 01*0.15 10*0.3 01*0.15 04*0
05*0 01*0.15 08*0.3 01*0.15 05*0
06*0 01*0.15 06*0.3 01*0.15 06*0
07*0 01*0.15 04*0.3 01*0.15 07*0
08*0 01*0.15 02*0.3 01*0.15 08*0
09*0 01*0.15       01*0.15 09*0

/
EQUALS
    'DZ'    20       1  20  1  10  1  1  /
    'PERMX' 500      1  20  1  10  1  1  /
    'TOPS'  4000     /

/     EQUALS IS TERMINATED BY A NULL RECORD

-- THE Y AND Z DIRECTION PERMEABILITIES ARE COPIED FROM PERMX
--   SOURCE  DESTINATION  ------- BOX ------
COPY
    'PERMX'   'PERMY'   1  20  1  10  1  1  /
    'PERMX'   'PERMZ'   /
/
RPTGRID
1 1 1 1 1 0 0 0 /
```

```
DEBUG
 0 0 1 0 1 0 1  /

PROPS    ================================================================

SWFN
   0.22    .0        0
   0.24    .002332   0
   0.32    .04225    0
   0.37    .087658   0
   0.42    .147124   0
   0.52    .305245   0
   0.57    .402858   0
   0.62    .512316   0
   0.72    .765554   0
   0.8     1         0
/
SOF2       1 TABLES   20 NODES IN EACH          FIELD   13:34  5 MAY 85
   .20     .0000
   .28     .019025
   .38     .096314
   .43     .157253
   .48     .233056
   .58     .429251
   .63     .549643
   .68     .684899
   .76     .932224
   .78     1
/

PVTW
  .0  1.0  3.03E-06  1  0.0 /

PVDO
  .0     1.0     1
 8000.0   .92    1
/
ROCK
 4000.0         .30E-05 /

DENSITY
 52.0000  64.0000   .04400 /

RPTPROPS
   2*0 /

REGIONS    ================================================================

SATNUM
 200*1 /

SOLUTION   ================================================================

EQUIL
4000  4000  6000  0   0   0   0   0   0  /
```

```
RPTSOL
1 0 1 /

SUMMARY  ============================================================

--REQUEST PRINTED OUTPUT OF SUMMARY FILE DATA


WOPR
/
WWPR
/
WWCT
/
WWIT
/

RUNSUM

SEPARATE

RPTSMRY
 1  /

SCHEDULE  ============================================================

TUNING
10  25  /
1.0 0.5 1.0E-6  /
/
WELSPECS
'INJECTOR' 'G'   20  1  4000  'water'  /
'PRODUCER' 'G'    1  1  4000  'OIL'  /
/
COMPDAT
'INJECTOR'  20  1 1  1 'OPEN'   0  .0   0.5 /
'PRODUCER'   1  1 1  1 'OPEN'   0  .0   0.5 /
/
WCONPROD
'PRODUCER' 'OPEN' 'lRAT' 1*     1*     1*   100   1*   1*  /
/
WCONINJE
'INJECTOR' 'WAT' 'OPEN' 'RATE' 100 /
/
TSTEP
20*365
/

END
```

VITA

Name:	Ruslan Guliyev
Address:	Department of Petroleum Engineering Texas A&M University College Station, TX 77843-3116
Email Address:	rguliyev202@yahoo.com
Education:	B.S., Petroleum Engineering, Azerbaijan State Oil Academy, 2002. M.S., Petroleum Engineering, Texas A&M University, 2008.
Employment History:	Schlumberger, Wireline Engineer, CAG, 2002-2004 Internship in BP Azerbaijan, Azeri Base Management Team. 2005.